Biomedicine & Pharmacotherapy 186 (2025) 117990

Contents lists available at ScienceDirect

Biomedicine & Pharmacotherapy

journal homepage: www.elsevier.com/locate/biopha

The anti-atherosclerotic effect of chronic AT1 receptor blocker treatment also depends on the ACE2/Ang(1−7)/Mas axis

Tobias Klersy [a,1], Leonie Achner [a,1], Benedikt Fels [b], Flavia Rezende [c,d], Melina Lopez [c,d], Natalia Alenina [e], Frauke Spiecker [a], Ines Stölting [a], Walter Häuser [a], Tobias Reinberger [f,g], Zouhair Aherrahrou [f,g], Carsten Kuenne [h], Carl Vahldieck [b], Urte Matschl [i], Susanne Hille [g,j], Michael Bader [e,k,l,m], Ralf P. Brandes [c,d], Oliver J. Müller [g,j], Kristina Kusche-Vihrog [b,g], Walter Raasch [a,g,n,*]

[a] Institute for Experimental and Clinical Pharmacology and Toxicology, University of Lübeck, Germany
[b] Institute for Physiology, University Lübeck, Germany
[c] Institute for Cardiovascular Physiology, Faculty of Medicine, Goethe-University Frankfurt, Germany
[d] DZHK (German Center for Cardiovascular Research) Partner site Rhine-Main, Germany
[e] Max-Delbrück-Center for Molecular Medicine (MDC), Berlin, Germany
[f] Institute for Cardiogenetics, University Lübeck; University of Lübeck, Germany
[g] DZHK (German Centre for Cardiovascular Research), partner site Hamburg/Kiel/Lübeck, Germany
[h] Department of Cardiac Development and Remodeling, Max Planck Institute for Heart and Lung Research, Bad Nauheim, Germany
[i] Department Virus Immunology, Leibniz Institute for Virology, Hamburg, Germany
[j] Department of Internal Medicine V, University Hospital Schleswig-Holstein, Campus Kiel, Germany
[k] DZHK (German Centre for Cardiovascular Research), partner site, Berlin, Germany
[l] Center for Structural and Cell Biology in Medicine, Institute for Biology, University of Lübeck, Lübeck, Germany
[m] Charité - University Medicine Berlin, Berlin, Germany
[n] CBBM (Centre for Brain, Behavior and Metabolism), University of Lübeck, Germany

ARTICLE INFO

Keywords:
Atherosclerosis
AAV-PCSK9^{DY} mouse model
Atomic force microscopy
Cortical stiffness

ABSTRACT

Blockade of AT_1-receptors by telmisartan (TEL) has anti-atherosclerotic efficacy. We investigated to what extent the ACE2/Ang1–7/Mas axis-dependent mechanism contributes to the TEL-induced protection of endothelial function.

Abbreviations: AAV-PCSK9, pro-protein convertase subtilisin/kexin type 9; Abcg1, ATP-binding Cassette Sub-family G Member 1; ACE2, Angiotensin converting enzyme 2; AFM, Atomic Force Microscopy; Ang II, Angiotensin II; Ang1-7, Angiotensin 1–7; ApoE, apolipoprotein E; ARBs, AT1 receptor blockers; AT1R, Angiotensin II receptor subtype 1; ATP, Adenosine triphosphate; Bw, body weight; Cpn2, Carboxypeptidase N Subunit 2; Cpt1b, Carnitine Palmitoyltransferase 1B; Cyp1a1, Cytochrome P450 1A1; Dio2, Iodothyronine Deiodinase 2; ECM, extracellular matrix; EG, endothelial glycocalyx; ENOS, endothelial nitric-oxide synthase; Fam20c, family with sequence similarity 20, member C; FCS, fetal calf serum; HA, Hyaluronan; Hdac11, Histone Deacetylase 11; Hk2, hexokinase 2; HOMA, Homeostasis Model Assessment; Hsd17b6, hydroxysteroid 17-beta dehydrogenase 6; Il10, Interleukin-10; Il12, Interleukin-12; Il6, Interleukin-6; INFγ, Interferon-gamma; Isyna1, Inositol-3-Phosphate Synthase1; Kc, Keratinocyte chemoattractant; Ko, knock out; LDL, Low-Density-Lipoprotein; LIX, Lipopolysaccharide-induced Cxc chemokine; Mac-1, Macrophage-1 antigen; Mcp1/Ccl2, Monocyte chemoattractant protein; Mep1b, meprin A, beta; MIP2, Macrophage inflammatory protein; Mmp12, Matrix Metallopeptidase 12; Mmps, Matrix Metallopeptidases; Mtor, mechanistic target of rapamycin; Myh1, muscle myosin heavy chain 1; Nfkβ, nuclear factor kappa B; NO, nitric oxide; Npc1l1, Npc1 Like Intracellular Cholesterol Transporter 1; Npr3, Natriuretic Peptide Receptor 3; Nr1I2, Nuclear Receptor Subfamily 1 Group I Member 2; ORO, Oil Red-O; PCA, Principal component analyses; PDGF, platelet-derived growth factor; PG, prostaglandin; Plin5, Perilipin-5; Pon1, Paraoxonase 1; PPARα, Peroxisome proliferator-activated receptor-alpha; PPARγ, Peroxisome proliferator-activated receptor-gamma; Pvalb, Parvalbumin; PYY, peptide tyrosine tyrosine; Rbl1, Retinoblastoma-like protein 1; Ren1, renin 1; Rgs2, Regulator Of G Protein Signaling 2; RNAseq, RNA sequenzing; ROS, reactive oxygen species; S100b, S100 calcium-binding protein B; SD, standard deviation; Slc15a1, solute carrier family 15, member 1; Slc24a3, Solute Carrier Family 24 Member 3; TC, total cholesterol; TEL, telmisartan; TG, triglyceride; Tnfα, Tumor Necrosis Factor-alpha; Tnntl3, Troponin I3, Cardiac Type; Trim31, ripartite Motif-containing Protein 31; Vcam-1, vascular cell adhesion protein 1; VSMC, vascular smooth muscle cell; WD, western diet.

* Correspondence to: Institute of Experimental and Clinical Pharmacology and Toxicology, University of Lübeck, Ratzeburger Allee 160, Lübeck 23538, Germany.
E-mail address: walter.raasch@uni-luebeck.de (W. Raasch).

[1] These authors made equal contributions and should both be considered as "first author".

https://doi.org/10.1016/j.biopha.2025.117990
Received 16 January 2025; Received in revised form 6 March 2025; Accepted 13 March 2025
Available online 18 March 2025

Endothelial dysfunction
Telmisartan
AT_1 receptor blockade
ACE2
Angiotensin(1−7)
Mas receptor
Matrix Metallopeptidase 12

Atherosclerosis was induced in C57BL/6 N, Mas-knock out (ko), and Ace2-ko mice by AAV-PCSK9^{DY} (2×10^{11} VG) injections plus Western diet (WD) feeding (12w). Mice were treated (12w) with TEL or vehicle. Controls received no PCSK9^{DY}, chow-feeding, and vehicle-treatment. In the aortae of mice, the plaque burden was determined, RNAseq analyses were performed and functional properties were assessed by quantifying the mechanical properties of the endothelial surface by Atomic Force Microscopy.

Regardless of strain, plaque burden and total cholesterol were increased upon AAV-PCSK9^{DY}+WD but decreased by TEL. Cortical stiffness was also enhanced in all strains by AAV-PCSK9^{DY}+WD but reduced under TEL only in the C57BL/6 N, while remaining still high in both knockout strains. Plasma NO negatively correlated with cortical stiffness in C57BL/6 N, but not in transgenic mice. TNFα plasma levels and aortic MMP12 expression was increased in PCSK9^{DY}/WD vehicle-treated controls and was normalized by TEL in C57BL/6 N but not in Mas-ko and Ace2-ko mice.

We conclude that TEL-induced reduction of endothelial stiffness occurred only in the C57BL/6 N but not in the Mas-ko and Ace2-ko mice. We suggest that the protective TEL effect is partly due to an Ang(1−7)/ACE2/Mas axis mediated mechanism. Since Mmp12 has well-known proatherogenic properties but was not altered in the two transgenic mouse lines, follow-up studies are required to further elucidate the correlation between Mmp12 and the Ang(1−7)/ACE2/Mas axis with respect to atherosclerosis.

AT_1 receptor blockers (ARBs) are established in the therapy of hypertension and heart failure. Beyond that, they reduce body weight, energy intake, fat mass, adipocyte size, and plasma concentrations of leptin in rats, mice, and humans, but increase energy expenditure [1,2]. These anti-obesity effects are also detectable in rats with diet-induced obesity (DIO) when the ARB was administered in a curative treatment setting [3], but they are only observed when ARBs are administered at high doses and are independent of their antihypertensive effects [3,4]. The underlying mechanisms have also not been conclusively elucidated to date, however, it seems that several mechanisms are involved, as we have previously demonstrated that leptin-dependent [4–6], cerebral [7–9], gastral [10,11], and ACE2/Angiotensin(1−7)/Mas-dependent mechanisms [12–17] are involved, whereas the pleiotropic ARB effects, namely PPARγ stimulation [2,6] or stress-reducing potential [18], are of no or only minor importance for the anti-obesity effects of ARBs.

The fourth cardinal symptom of the metabolic syndrome besides insulin resistance, hypertension, and obesity, is hyperlipidemia, thus being a high-risk factor for atherosclerosis. While stimulation of the ACE/Angiotensin II/AT_1 receptor axis leads to accelerated atherosclerosis development [19,20], ARB therapy has been clinically shown to attenuate vascular dysfunction [21]. Also, stimulation of the ACE2/Ang (1−7)/Mas axis tends to have a preventive effect against the development of atherosclerosis and endothelial dysfunction [22–24]. Thus, Ang (1−7) oppose the actions of ANG II directly or as a result of increasing nitric oxide (NO) or prostaglandins (PGs) [25] and reduces atherosclerotic lesions in apolipoprotein E (ApoE)-ko mice [26]. In contrast, genetically induced ACE2 deficiency [with consecutive decreased Ang (1−7) biosynthesis] accentuates pro-inflammatory and pro-atherosclerotic vascular effects [27], while overexpression of ACE2 leads to a reduction in the intimal thickness of vessels and stabilization of atherosclerotic processes [28]. Compared with high-fat-fed ApoE-ko mice, Mas/ApoE-dko mice were shown to have increased expression of proinflammatory interleukins, accumulation of mononuclear cells, and also increased aortic lesion area [29].

To test the functional significance of the ACE2/Ang(1−7)/Mas axis for ARB-induced anti-atherosclerotic efficacy, we here used both Mas-ko and Ace2-ko transgenic mice. Induction of atherosclerosis in mice requires either the use of ApoE-ko, LDL receptor-ko, or ApoE/LDL-R dko transgenic mice or injection of AAV-PCSK9^{DY} [pro-protein convertase subtilisin/kexin type 9 (PCSK9)-adeno associated virus (AAV)] [30]. In 2014/15, it was reported for the first time that a single injection of AAV-PCSK9^{DY} in combination with a cholesterol-rich diet resulted in a doubling of serum cholesterol concentration after only 30 days and that this concentration remained stably elevated over the period of one year [31,32]. As a result of hyperlipidemia after AVV-PCSK9^{DY}-injection, the mice developed full-blown atherosclerosis (development of plaques, macrophages infiltration, formation of foam cells, fibrosis, formation of lesions) in a dose-dependent manner [31–35]. By using the Atomic Force Microscope (AFM) as a nanoindentation tool, we recently confirmed such findings and further observed that mechanical stiffness of the endothelial surface was increased in Atomic Force M*icroscopy* (AFM) studies, suggesting endothelial dysfunction in response to AVV-PCSK9^{DY} injection [36].

In previous studies, we could demonstrate that the mechanical properties of the endothelial cell surface, including the endothelial glycocalyx (EG) and the cortex, an actin-rich layer 150–200 nm beneath the plasma membrane, are crucial for the proper function of the vascular endothelium [37]. Since the stiffness is directly linked to the release of NO from the endothelial cells, which leads to the relaxation of the vascular smooth muscle cells and, thus, to a decreased vascular tone, it can be seen as a hallmark of endothelial (dys)function. In fact, stiffening of the cortex, deterioration of the glycocalyx and reduced bioavailability of NO were found in inflammatory conditions including atherosclerosis. Of note, endothelial stiffening could be correlated with arterial stiffness in patient cohorts [38,39].

As atherosclerosis and arterial stiffness are interrelated and further provoke other cardiovascular events [40], the aim of the current study was to investigate whether endothelial cell stiffness was increased in the AAV-PCSK9^{DY} model but normalized by the ARB telmisartan. We further aimed to investigate whether this protective TEL-induced antiatherosclerotic effect is rather caused by its AT_1 receptor antagonistic effect or whether it could also be explained by a stimulation of the ACE2/Ang (1−7)/Mas axis. This hypothesis is based on the well-established knowledge that the AT_1 receptor-based negative feedback is abolished by ARB blockade, thus consequently stimulating the renin activity and increasing not only AngII [2,3] but also Ang(1−7) [41,42] (see also Fig. S1). To pursue this goal, we used Mas-ko and Ace2-ko mice and hypothesized that the antiatherosclerotic effect would not be detectable or at least only partially detectable in Mas- or Ace2-deficient mice, respectively, which would then suggest an ACE2/Ang(1−7)/Mas axis-dependent mechanism. In addition to the functional characterization of the mechanical cell properties by AFM, we determined aortic gene expression as a consequence of atherosclerotic changes and TEL treatment.

1. Methods

1.1. AAV vector production and purification

AAV serotype 8 vectors for expression of the murine D377Y-PCSK9 cDNA (AAV-PCSK9^{DY}) were produced as previously described [43] by using the two-plasmid method and cotransfecting AAV/D377Y-mPCSK9 (gift from Jacob Bentzon; Addgene plasmid # 58376) [31] together with the helper plasmid pDP8 [44] in HEK293T cells using polyethyleneimine (Sigma Aldrich). AAV vectors were purified using iodixanol step gradients and titrated as previously described [45]. In the

following, we denote this vector as AAV-PCSK9^{DY}.

1.2. Animals

All animal care and experimental procedures were conducted in accordance with the NIH guidelines for the care and use of laboratory animals and were approved by the local animal ethics committee (Ministerium für Energiewende, Landwirtschaft, Umwelt, Natur und Digitalisierung des Landes Schleswig-Holstein, Germany) under the application number V241–60532/2017(75–7/19, 85–9/18). The results of all studies involving animals are reported in accordance with the ARRIVE guidelines [46]. The group sizes of n = 12 in each group were assessed by a power analysis (corrected α = 0.01, power 80 %) by considering TEL-induced weight gain regulation [6–8,47]. In total, 108 mice were used for this study. Male Mas-ko (Mas1tm1Bdr) [48] and Ace2-ko (B6.129P2/OlaHsd-Ace2tm1Pgnr) mice [49,50] were used in the experiments with an initial age of 10–11 weeks. The effectiveness was convincingly demonstrated in the initial description of both transgenic mouse lines [48–50] and, for the Mas-ko mice, also by ourselves after initial introduction of the mice into our breeding unit [51]. The Mas- and Ace2-deficient mice were bred on a C57BL/6 N background in the lab of Michael Bader (Max Delbrück Center for Molecular Medicine, Berlin) and imported via homozygous embryo transfer to the Animal Facility in Lübeck, where own breeding of these transgenic mice was established. Ten/eleven-week-old male C57BL/6 N mice (Janvier Labs, Germany) were used as controls. All mice were kept in standard housing in groups of 2–4 individuals randomized by weight. Mice had ad libitum access to a standard chow diet for a 2-week habituation period before starting the study and receiving the AAV-mPCSK9^{DY} injections. In order to prevent false high levels in the nitrite determination, the drinking water was changed to low nitrite/nitrate water one week before the end of the study. One Ace2-ko mouse in the PCSK9^{DY}/WD+VEH group died for unknown reasons and one Ace2-ko mouse from PCSK9^{DY}/WD+TEL was excluded from the evaluations because weight gain of this animal was abnormal.

1.3. Mouse experiments

Mice were injected with AAV-PCSK9^{DY} (2×10^{11} VG in 100 µl) or with 100 µl saline via the tail vein at an age of 10 weeks. Afterwards, AAV-PCSK9^{DY}-treated mice were fed a Western diet (WD, EF TD88137 mod. +1.25 % Cholesterol, ssniff Spezialdiäten GmbH) for 3 months [36], while the saline-treated controls received standard chow. One of each PCSK9^{DY}/WD-fed group of Mas-ko, Ace2-ko and C57BL/6 N mice, respectively, was treated with TEL (8 mg/kg$_{bw}$, once per day by gavage) whereas the other groups served as controls, all receiving an identical volume of vehicle (5 ml per 1 kg$_{bw}$/d) instead of TEL (Tab. S1). Seven days before virus injection and at the end of the study approx. 100 µl EDTA-blood was withdrawn retro-orbitally. Body weight was monitored daily, as the TEL dose was dependent on this. Body composition was measured at week 11 with the Minispec BCA analyzer (LF-110, Bruker) 2 h after the mice were transferred to the room to acclimatize to the environment. For the measurements, mice were put into the restrainer, which was then placed in the analyzer [7,36,52]. After 12 weeks, the animals were anesthetized (intraperitoneal injection of 0.6–1 ml of a solution of 0.7 ml ketamine (100 mg/ml), 0.7 ml xylazine (2 %) and 8.6 ml saline) for final blood sampling by intracardiac (to obtain hemolysis-free samples for plasma nitrite determination) and retroperitoneal puncture. Afterwards, mice were sacrificed by cervical dislocation. This was followed by intracardiac blood sampling to obtain hemolysis-free samples for plasma nitrite determination. Aortas (from the aortic root to the iliac bifurcation) were removed, after which fat and connective tissue were trimmed. Thoracic aorta was divided into 3 segments. One part was immediately used for AFM measurements, the second was fixed in 4 % paraformaldehyde solution and then used for histological analysis (plaque lesion analysis) and the third was snap frozen and stored at −80°C for RNAseq analyses (Tab. S2).

1.4. Quantification of the mechanical properties by AFM in aortic endothelial cells

Mouse aortas were isolated and trimmed from surrounding tissue. A small patch (≈1 mm^2) of the whole aorta was removed and attached on Cell-Tak (BD Biosciences, Bedford, MA, USA) coated slide, with the endothelial surface facing upward and cultured at 37 °C and 5 % CO_2 in minimal essential medium (MEM; Invitrogen, Life Technologies,Carlsbad, CA, USA), containing 10 % fetal calf serum (FCS; PAA Laboratories, Pasching, Austria, 1 % MEM vitamins (Biochrom, Ltd., Cambridge, United Kingdom), penicillin G (10,000 U/ml), streptomycin (10,000 mg/ml), and 1 % MEM nonessential amino acids (MEM NEAA; Gibco, Life Technologies) [53]. 24 h and 48 h after aortas were prepared the mechanical properties were determined by using the AFM-based nanoindentation measurements as described elsewhere [36,54–57]. For AFM measurements, a cantilever (Novascan Technologies, Boone, North Carolina, United States) with a mounted spherical tip (diameter 10 µm) and nominal spring constants of 10 pN/nm (glycocalyx) and 30 pN/nm (cortex)were used. A maximal loading force of 4.5 nN was applied and force-distance curves were created in 8-fold replicates on 37–50 cells in each mouse. These AFM data were collected with Research NanoScope Software (version 9.20 (Bruker 2016); 2). The slope of this force-deformation curve then directly reflects the force (in nano Newton), here defined as stiffness, that must be exerted to indent the cell for a certain distance. The height and stiffness values of eGC and cortical actin were calculated from force-deformation curves (Fig. 3A) using the Protein Unfolding and Nano-Indentation Analysis Software Punias 3D (Version 1.0; Release 2.3; Copyright 2009).

1.5. Histological analysis

For all atherosclerotic plaque analyses, investigators were blinded. As described previously [36,58,59], serial cross-Section (8- to 10-µm thick) were obtained, starting below the aortic root to the proximal aorta, below the aortic arch. The sections were stained using Oil Red-O (ORO) and the mean atherosclerotic lesion area was calculated from 8 to 10 sections at 40 µm intervals, starting at the appearance of at least two aortic valves until the aortic valves disappeared. Images were acquired using a Keyence microscope (BZ-X800). Sections were manually cropped using GIMP software, version 2.6 (The GIMP Development Team) to yield aortic root areas [36]. Areas of lesions and ORO-positive regions were determined using an in-house Python script (available on request). In brief, the Python package OpenCV () was utilized to process images and to determine lesions based on color thresholds (e.g., reddish pixel for ORO). The ratio of ORO-positive lesions in each animal was determined as the percentage lesion area, normalized to the total area of the aorta.

1.6. Total Cholesterol (TC) and Triglyceride (TG) analyses

Plasma was prepared by centrifugation. Plasma concentrations of TC (EnzyChrom HDL/LDL/VLDL Assay Kit 100 T, from Biotrend Chemikalien GmbH, Germany) and TG (Triglyceride ColorimetricAssayKit 96well from Biomol GmbH, Germny) were analyzed in the mice as described previously [58] to study whether an increasing viral load affects lipid profiles.

1.7. Plasma Nitrite

Accordant to previous reports [60], nitrite was measured in plasma of mice as a footprint of NO with an NO analyser (Sievers NOA-280) apparatus using acetic acid and sodium iodide (AppliChem #A1887) in a nitrogen atmosphere. Plasma was further cleared by centrifugal filter units (Microcon®-10, Merck #MRCPRT010) for 70 min at 14,000 g

at 4 °C, and 50 µl were loaded into the NO analyzer.

1.8. Blood cytokine analysis

Blood glucose was measured using a commercial glucose sensor (Accu-Chek® Performa, and Glucose Sensors Inform II, Roche, Germany). Plasma concentrations of diverse adipocytokines were measured in 10 µL of sample by immunosorbent assays according to the manufacturer's instructions using the Milliplex mouse metabolic magnetic bead panel kit MMHMAG-44K.mouse (Amylin Active, C-Peptide 2, Ghrelin, GIP, GLP-1 Active or GLP-1 Total, Glucagon, Il-6, Insulin, Leptin, Mcp-1, PP, PYY, Resistin, Secretin, and Tnfα), and Mhstcmag-70K (Gm-Csf, Infγ, Il-1α, Il-1β, Il-2, Il-4, Il-5, Il-6, Il-7, Il-10, Il-12 (p70), Il-13, Il-17A, Kc/Cxcl1, Lix, Mcp-1, Mip-2, Tnf-α) from Millipore (Germany).

1.9. RNA sequencing

RNA sequencing (RNAseq) analysis was performed from the descending aorta. Aortic tissue was isolated, trimmed from fat, and snap frozen in liquid nitrogen. For the RNAseq analyses, the aortic segments of 3mice were pooled and a total of 4 sampleswere analyzed. This means that the results represent 12 mice used each group. Total RNA was isolated with the RNA Mini Kit from Bio& SELL (Nuremberg, Germany) combined with on-column DNase digestion (DNase-Free DNase Set, Qiagen) to avoid genomic DNA contamination. RNA and library preparation integrity were verified with LabChip Gx Touch 24 (Perkin Elmer). As input for VAHTS Stranded mRNA-seq Library preparation, 500 µg of total RNA was used following the manufacturer's protocol (Vazyme). Sequencing was performed on a NextSeq2000 instrument (Illumina) with 1x72-bp single-end setup. The resulting raw reads were assessed for quality, adapter content, and duplication rates with FastQC (RRID:SCR_014583) (Andrews Simon: Andrews Simon: FastQC: a quality control tool for high-throughput sequence data. Available online at http://www.bioinformatics.babraham.ac.uk/projects/fastqc).

1.10. RNA sequencing analysis

Trimmomatic version 0.39 was employed to trim reads after a quality drop below a mean of Q15 in a window of 5 nucleotides and keeping only filtered reads longer than 15 nucleotides [61]. Reads were aligned versus Ensembl mouse genome version mm10 (Ensembl release 101) with STAR 2.7.10a [62]. Aligned reads were filtered to remove duplicates with Picard 2.27.4 (Picard: A set of tools in Java for working with next-generation sequencing data in the BAM format), multi-mapping, ribosomal, or mitochondrial reads. Gene counts were established with featureCounts 2.0.4 by aggregating reads overlapping exons on the correct strand, excluding those overlapping multiple genes [63]. The raw count matrix was normalized with DESeq2 version 1.36.0 [64]. Contrasts were created with DESeq2 based on the raw count matrix. Genes were classified as significantly differentially expressed at average count > 5, multiple testing adjusted p-value < 0.05, and log2FC $< -0.585 <$ or log2FC > 0.585. The Ensemble annotation was enriched with UniProt data (Activities at the Universal Protein Resource (UniProt)).

To identify a potential association of genes with atherosclerosis, we used the CTD Gene-Disease Associations dataset (date of last database check: 07/23/2024) [65], (https://maayanlab.cloud/Harmonizome/gene_set/Atherosclerosis/CTD+Gene-Disease+Associations) [66]. In the following tables, we have quoted the standardized value determined there, which indicated the relative strength of the functional associations.

1.11. Statistical analysis

GraphPad Prism 8.0 (La Jolla, USA) was used for statistical analysis. All data were checked for outliers and were tested for Gaussian distribution and variance homogeneity. For the statistical analysis, we chose a tiered procedure: First, we compared the C57BL/6 N, Mas-ko, and Ace2-ko mice under chow diet to detect possible strain differences. Subsequently, a 1-way ANOVA followed by Tukey's multiple multiple comparisons test was used for comparing different groups, assuming a Gaussian distribution and variance homogeneity. In case of no variance homogeneity, a Brown-Forsythe ANOVA test was used, followed by a Dunnett's T3 multiple comparisons test. Alternatively, if the Gaussian distribution was not given, we used the Kruskal Wallis Test followed by Dunn's multiple comparisons tests. Correlation analyses were performed by applying the 1- or 2-tailed. Correlation analyses were performed by applying the 1- or 2-tailed Pearson test. A p-value < 0.05 was considered statistically significant. Inbox graphs (representing the 25th to 75th percentiles) with whiskers (representing the maximum and minimum values), both the individual data and the medians are presented. In the line graphs, means ± SDs are depicted.

2. Results

2.1. Growth and glucose homeostasis

For reasons of clarity, only the most important findings on the regulation of growth and glucose homeostasis are summarized here; for a detailed presentation and discussion, please refer to the Supplemental Data. WD feeding induced increase in body weight, fat mass and plasma leptin in C57BL/6 N and Mas-ko, thus clearly indicating development of obesity which was prevented in both strains by TEL. In contrast, Ace2-ko mice on WD feeding did not develop obesity and TEL treatment even reduced body weight to levels below chow controls (Fig. 1A-C; Figs. S2–4, Tabs S3–4). As a result of the PCSK9DY^{DY}/WD intervention, insulin sensitivity was at least slightly impaired in the C57BL/6 N mice, In the Mas ko mice, however, this was more clearly affected, the HOMA index was increased under VEH treatment, but was normalized again by TEL administration. In contrast, we observed no influence in the Ace2-ko mice (Fig. 1D, Figs. S5/6, Tabs S5/6). Only in C57BL/6 N but not in the two transgenic mouse lines, TNFα and MIP2 were increased in response to the WD intervention. TEL treatment in C57BL/6 N prevented the increase in TNFα as well as MIP2. (Fig. 1E/F). Such a pattern (although not to this clarity or extent) was also seen with MCP1/CCL2, IL2p70, KC, LIX and IL6. (Fig. S7, Tabs S5).

2.2. Atherosclerotic lesions

Primarily, it is striking that in comparison to the C57BL/6 N mice, plasma cholesterol tended to be elevated in the Ace2-ko mice, whereas plasma triglyceride is decreased before any treatment at the age of 11 weeks. TG was slightly lower in the Mas-ko mice than in the C57BL/6 N controls (Tab. S3). Lower TG levels were still observed in chow-fed Ace2-ko mice at the end of the study (Tab. S5), indicating that in terms of lipid metabolism, the Ace2-ko behave differently to Mas-ko mice.

In response to the PCSK9^{DY}/WD intervention, plasma TC and plasma TG increased by a factor of 7–8 and 5–10, respectively, in all VEH-treated mice (Fig. 2D/E). In the C57BL/6 N mice, this TC increase was partially antagonized by TEL but not in the Mas-ko and Ace2-ko mice (Fig. 2D). Plasma TG remained nearly at the level of the VEH-treated C57BL/6 N controls even with Tel treatment and equally unaffected in the two transgenic mouse lines (Fig. 2E). Across all interventions, plasma cholesterol, plasma TG and plaque burden exhibited an almost perfect correction irrespectively of the mouse strains studied (Fig. 6).

Chow-fed controls developed no atherosclerotic plaques (Tab. S4). In response to PCSK9^{DY}/WD, both, plaque and fat content markedly increased. This increase was partially diminished by TEL in C57BL/6 N as well as in Mas-ko and Ace2-ko mice (Fig. 2B/C). Additional parameters (percentage plaque content, fat ratio in plaque, strong and light fat

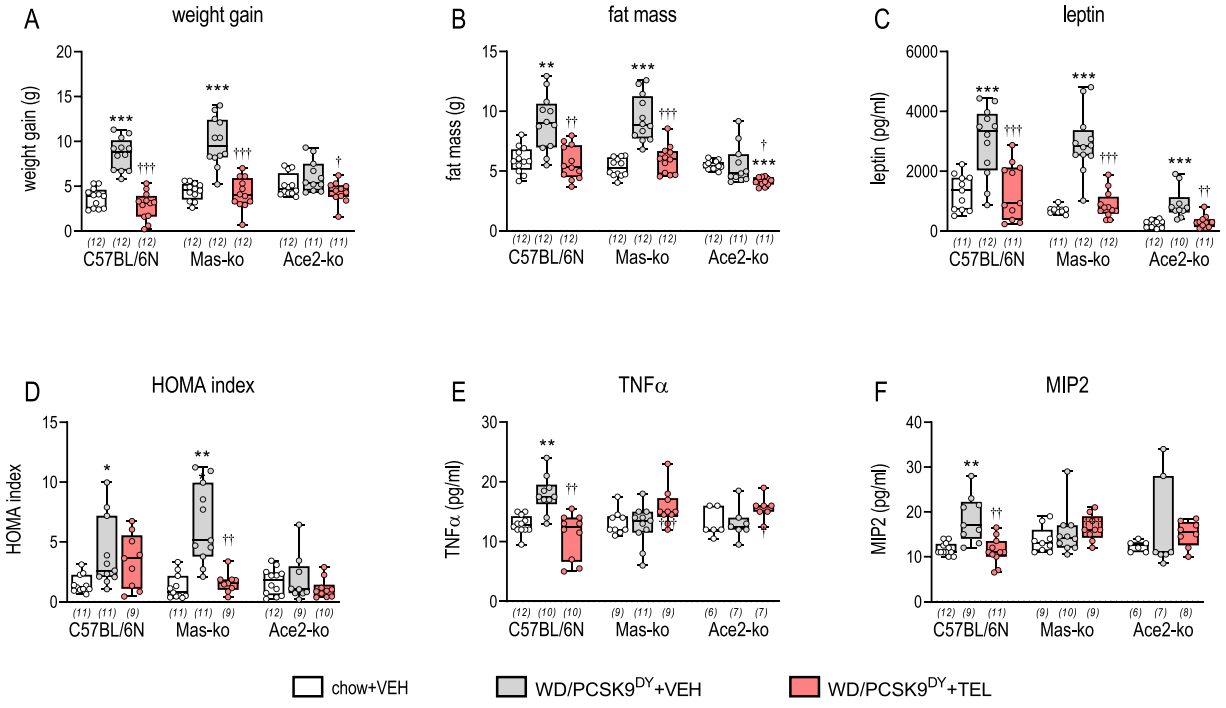

Fig. 1. Growth parameters of C57BL/6 N, Mas-ko and Ace2-ko mice in dependency of WD/PCSK9^{DY} and vehicle (grey bars) or TEL (red bars) treatment. Controls received chow and no PCSK9^{DY} (open bars). Weight gain (A), fat mass (B), plasma leptin (C), HOMA index, (D), plasma TNFα (E), and plasma MIP2 (F). A 1-way ANOVA followed by Tukey's multiple comparisons test was used for comparing different groups, assuming a Gaussian distribution and variance homogeneity. In case of no variance homogeneity, a Brown-Forsythe ANOVA test was used followed by a Dunnett's T3 multiple comparisons test. Alternatively, if the Gaussian distribution was not given, we used Kruskal Wallis Test followed by Dunn's multiple comparisons test. The median is depicted in box blots; the box extends from the 25th to 75th percentiles and the whiskers go down to the smallest value and up to the largest. The group size is indicated individually for each group in brackets below the X-axis. *, **, *** $p < 0.05$, 0.01 or 0.0001 vs. saline/chow plus VEH; †, ††, ††† $p < 0.05$, 0.01 or 0.0001 vs PCSK9^{DY}/WD plus VEH.

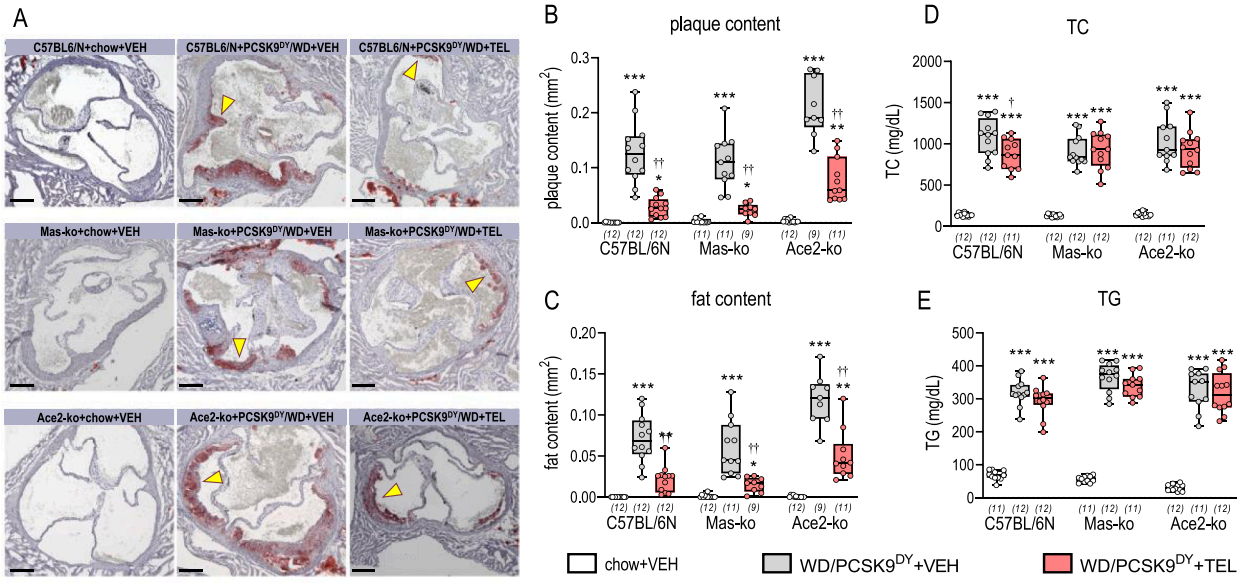

Fig. 2. Atherosclerotic changes in C57BL/6 N, Mas-ko and Ace2-ko mice in dependency of WD/PCSK9^{DY} and VEH (grey boxes) or TEL (red boxes) treatment. Chow-fed controls also received vehicle (open boxes). A: depicts exemplary aortic root segments of each treatment group upon Oil Red O staining (the brownish colorations marked with an arrow are plaques; scale bar: 100 μm); B: quantitative evaluation of plaque content; C: quantitative evaluation of fat content; D: TC plasma levels; E: TG plasma levels; A 1-way ANOVA followed by Tukey's multiple comparisons test was used for comparing different groups, assuming a Gaussian distribution and variance homogeneity. In case of no variance homogeneity, a Brown-Forsythe ANOVA test was used followed by a Dunnett's T3 multiple comparisons test. Alternatively, if the Gaussian distribution was not given, we used Kruskal Wallis Test followed by Dunn's multiple comparisons test. The median is depicted in box blots; the box extends from the 25th to 75th percentiles and the whiskers go down to the smallest value and up to the largest. The group size is indicated individually for each group in brackets below the X-axis. *, **, *** $p < 0.05$, 0.01 or 0.0001 vs. saline/chow plus VEH; †, ††, ††† $p < 0.05$, 0.01 or 0.0001 vs PCSK9^{DY}/WD plus VEH.

content), also characterizing the atherosclerotic lesions, clearly confirmed the effects of PCSK9^{DY}/WD intervention. They at least partially supports the idea that TEL lowers plaque burden in C57BL/6 N and also in Mas-ko mice, but only to a limited extent in Ace2 ko mice (Fig. S8).

2.3. Vascular dysfunction

As a functional parameter of vascular dysfunction, the mechanical properties of aortic ex vivo ECs were quantified in a total of 520–587 ECs per group (37–50 ECs in one aorta of each mouse). Even when statistical analysis was based on individual mice of each group, Mas-ko mice showed significant higher cortical stiffness compared to C57BL/6 N controls (Mas-ko: 1.386 ± 0.034 pN/nm vs. 1.314 ± 0.039 C57BL/6 N, P = 0.0035, see Tab. S4), while the stiffness of Ace2-ko mice was not altered (due to the higher variability, 1.352 pN/nm, P = 0.1408, see Table 2). The cortical stiffness was higher in PCSK9^{DY}/WD-treated C57BL/6 N mice than in chow-fed controls independent whether mice were treated with VEH, but it was reduced under TEL by approximately one third compared with PCSK9^{DY}/WD+VEH-treated mice, suggesting at least a partial protective effect of TEL (Fig. 3B). In both transgenic strains, cortical stiffness was not impaired by PCSK9^{DY}/WD-intervention or improved by TEL-treatment (Fig. 3B). In contrast to cortical stiffness, GC height was not different between the 3 mouse strains and was not altered by PCSK9^{DY}/WD intervention or TEL therapy (Fig. 3C). A slight negative correlation between stiffness of aortic ECs and glycocalyx

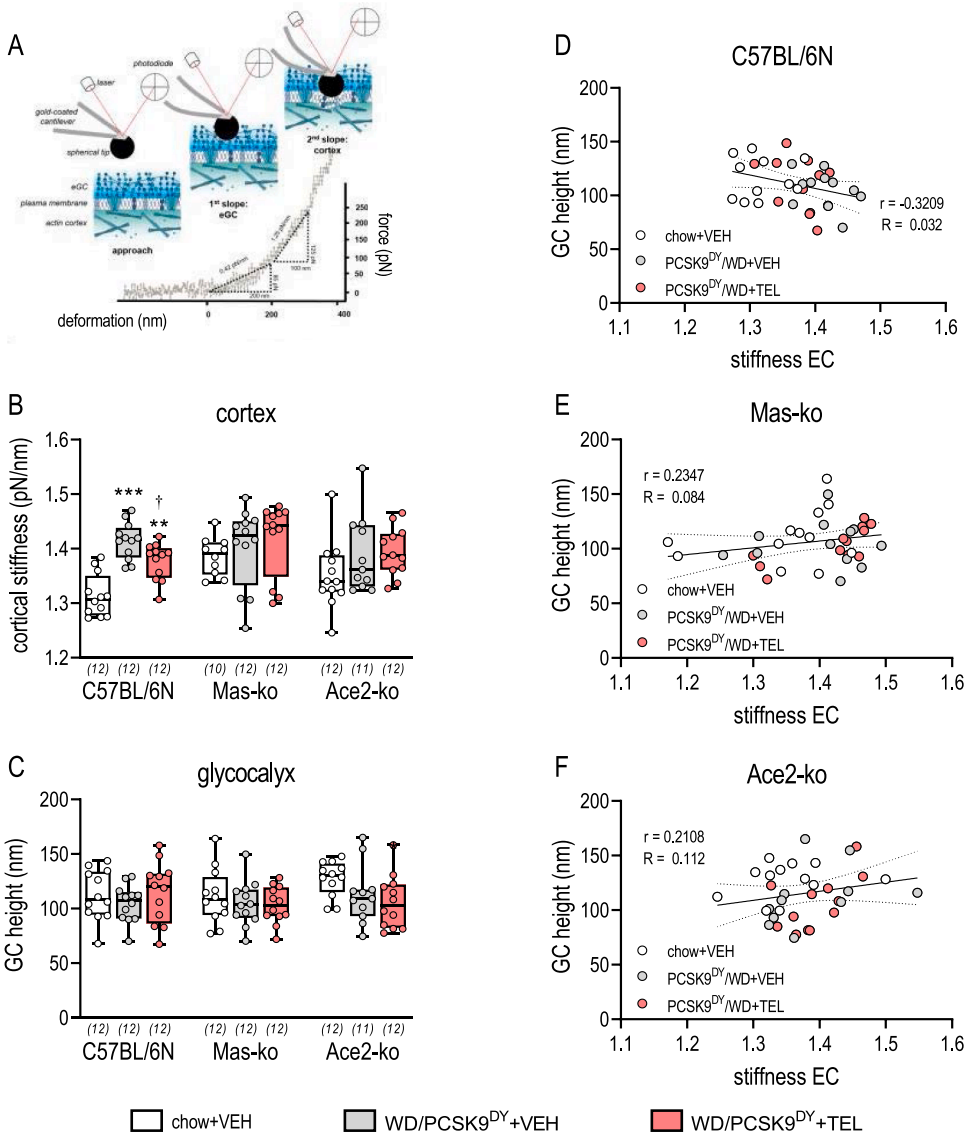

Fig. 3. Endothelial stiffness in C57BL/6 N, Mas-ko and Ace2-ko mice in dependency of WD/PCSK9^{DY} and VEH (grey boxes) or TEL (red boxes) treatment. Chow-fed controls also received vehicle (open boxes). Fig. A shows a schematic scheme for the force-deformation curve of the AFM investigation on which the evaluations of the stiffness of the endothelial cells (Fig. B) and the height of the glycocalyx (Fig C) were based. Pearson correlations (one-side) between stiffness of ECs and the height of glycocalix in C57BL6/N (D), Mas-ko (E) and Ace2-ko mice (F). Stiffness was calculated in 8-fold measurement repetition in 37–50 cells of each mouse from force-deformation curves in a blinded manner by using the PUNIAS 3D version 1.0 release 1.8 (http://punias.voila.net/). The mean value of the 37–50 cells was then calculated individually for each mouse. A 1-way ANOVA followed by Tukey's multiple comparisons test was used for comparing different groups, assuming a Gaussian distribution and variance homogeneity. In case of no variance homogeneity, a Brown-Forsythe ANOVA test was used followed by a Dunnett's T3 multiple comparisons test. Alternatively, if the Gaussian distribution was not given, we used Kruskal Wallis Test followed by Dunn's multiple comparisons test. The median is depicted in box blots; the box extends from the 25th to 75th percentiles and the whiskers go down to the smallest value and up to the largest. The group size is indicated individually for each group in brackets below the X-axis. *, **, *** $p < 0.05$, 0.01 or 0.0001 vs. saline/chow plus VEH; †, ††, ††† $p < 0.05$, 0.01 or 0.0001 vs PCSK9^{DS}/WD plus VEH.

height was observed in the C57BL/6 N mice, but not in the two transgenic mouse lines (Fig. 3D-F).

To confirm that vascular function was impaired in dependency on strain and/or atherosclerotic lesions, and if so, whether this dysfunction might be attenuated by TEL, we determined plasma nitrite as a surrogate parameter for NO. Plasma nitrite levels in chow-fed C57BL/6 N mice were 413±128 nM and these were halved in Mas-ko and tended ($P = 0.052$) to be lowered in Ace2-ko mice (Tab. S5). This finding suggests impaired endothelium-dependent vasodilation, at least for the Mas-ko mice, which would be in agreement with the results on cortical stiffness. As a result of the PCSK9^{DY}/WD intervention, plasma nitrite was tendentially ($P = 0.073$) reduced in the VEH-treated C57BL/6 N mice, and although not restored to normal or at least partially increased by TEL therapy (Fig. 4A). Such PCSK9^{DY}/WD or TEL effects were not observed in the transgenic mouse lines (Fig. 4A). However, correlation analyses not only reinforce the link between atherosclerotic lesions and functional vascular damage, but also highlight a functional disorder in the transgenic mouse lines. In C57BL/6 N mice cortical stiffness and plasma NO correlate negatively meaning, e.g. the higher the stiffness the lower the nitrite although, admittedly, the significance is borderline weak with a $p = 0.047$. (Fig. 5A). The key massage is that this negative correlation is not anymore observed in the Mas-ko or Ace2-ko mice (Fig. 5 B/C). Moreover, we observed a strong positive correlation between cortical stiffness on one side and TC (Fig. 5D), plaque content (Fig. 5G) and fat content (Fig. 5J) on the other side in C57BL/6 N controls (Fig. 6). And again, these positive correlations were also abolished in Ace2-ko or even reverted in the Mas-ko mice (Fig. 5/6). This suggests that the potency of TELin preventing atherosclerotic vascular dysfunction is partly due to an Ang(1−7)/ACE2/Mas-dependent effect.

The histological images of the ORO-staining also allow an evaluation of various vascular parameters. With the exception of the aortic lumen, no strain effects were observed for diameter, lumen and media (Tab. S4). Media thickness was increased by appr. 30 % in PCSK9^{DY}/WD and vehicle treated C57BL/6 N compared to the chow controls, while such an effect was not seen in the corresponding TEL-treated PCSK9^{DY}/WD animals (Fig. 4B). Diameter and lumen were increased in the PCSK9^{DY}/WD-treated Mas-ko mice and TEL at least decreased media in these animals (Fig. 4B-D).(Fig. 6)

2.4. Gene regulation in abdominal aorta segments

PCA plots and volcano plots upon RNAseq analyses clearly showed strain differences between C57BL/6 N, Mas-ko and Ace2-ko mice (Figs. S9 and S10). PCA blots (Fig. 7) as well as volcano plots (Fig. S11) furthermore showed that genes were down- and up-regulated in all strains as a result of the PCSK9^{DY}/WD intervention as well as vehicle or TEL-treatment.

In the aortas of C57BL/6 N, Ace2-ko and Mas-ko mice 579, 652, and 250 genes respectively were differentially regulated between PCSK9^{DY}/WD/VEH and chow-fed/VEH interventions, being more genes up- than downregulated (C57BL/6 N: 510/69, Ace2-ko: 477/175, Mas-ko: 215/35). Based on these datasets, we identified 101 genes that were regulated in all 3 strains by the PCSK9^{DY}/WD intervention, with the genes whose expression was most significantly altered shown in Fig. 8Aa and Tab. S7. Among these 101 genes, *Nr1I2, Ppara, Cpn2, Cpt1b* and *Isyna1* are associated with atherosclerosis according to the CTD Gene-Disease Associations dataset [65,66]. Strikingly, *Nr1I2* expression was up-regulated by the PCSK9^{DY}/WD intervention in the C57BL/6 N and Mas-ko, but down-regulated by the same amount in the Ace2-ko mice. (Fig. 9)

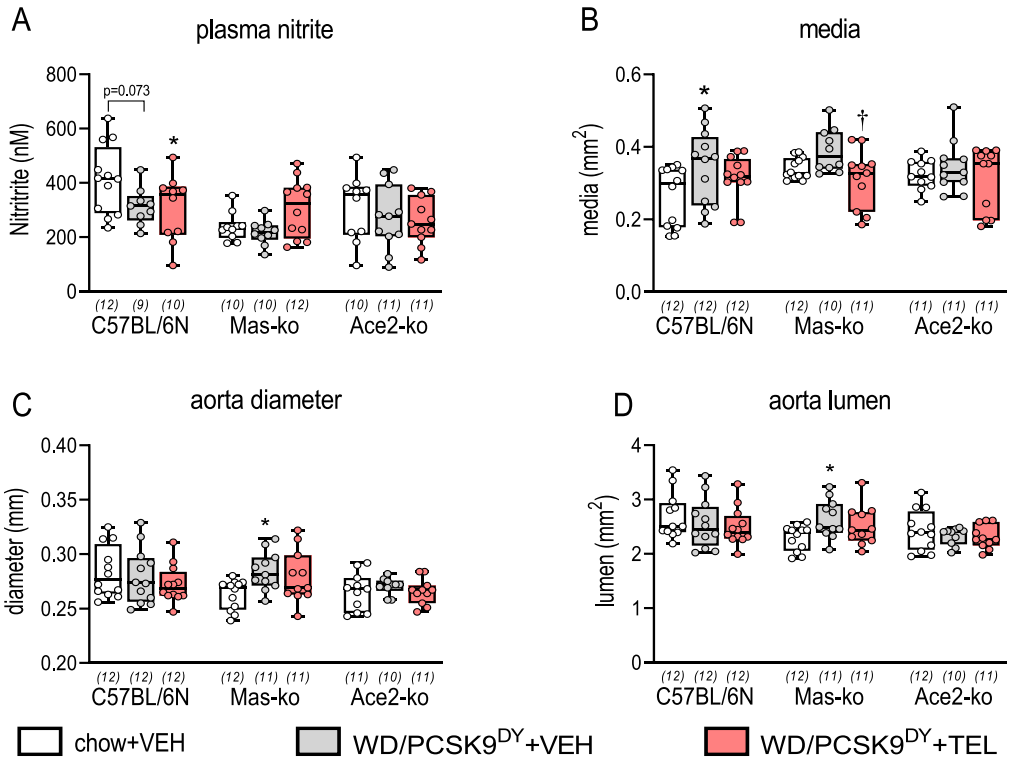

Fig. 4. Plasma nitrite levels (A), media (B); diameter (C) or lumen (D) of aortas of C57BL/6 N, Mas-ko and Ace2-ko mice in dependency of WD/PCSK9^{DY} and VEH (grey boxes) or TEL (red boxes) treatment. Chow-fed controls also received vehicle (open boxes). A 1-way ANOVA followed by Tukey's multiple comparisons test was used for comparing different groups, assuming a Gaussian distribution and variance homogeneity. In case of no variance homogeneity, a Brown-Forsythe ANOVA test was used followed by a Dunnett's T3 multiple comparisons test. Alternatively, if the Gaussian distribution was not given, we used Kruskal Wallis Test followed by Dunn's multiple comparisons test. The median is depicted in box blots; the box extends from the 25th to 75th percentiles and the whiskers go down to the smallest value and up to the largest. The group size is indicated individually for each group in brackets below the X-axis. *, **, *** $p < 0.05$, 0.01 or 0.0001 vs. saline/chow plus VEH; †, ††, ††† $p < 0.05$, 0.01 or 0.0001 vs PCSK9^{DS}/WD plus VEH.

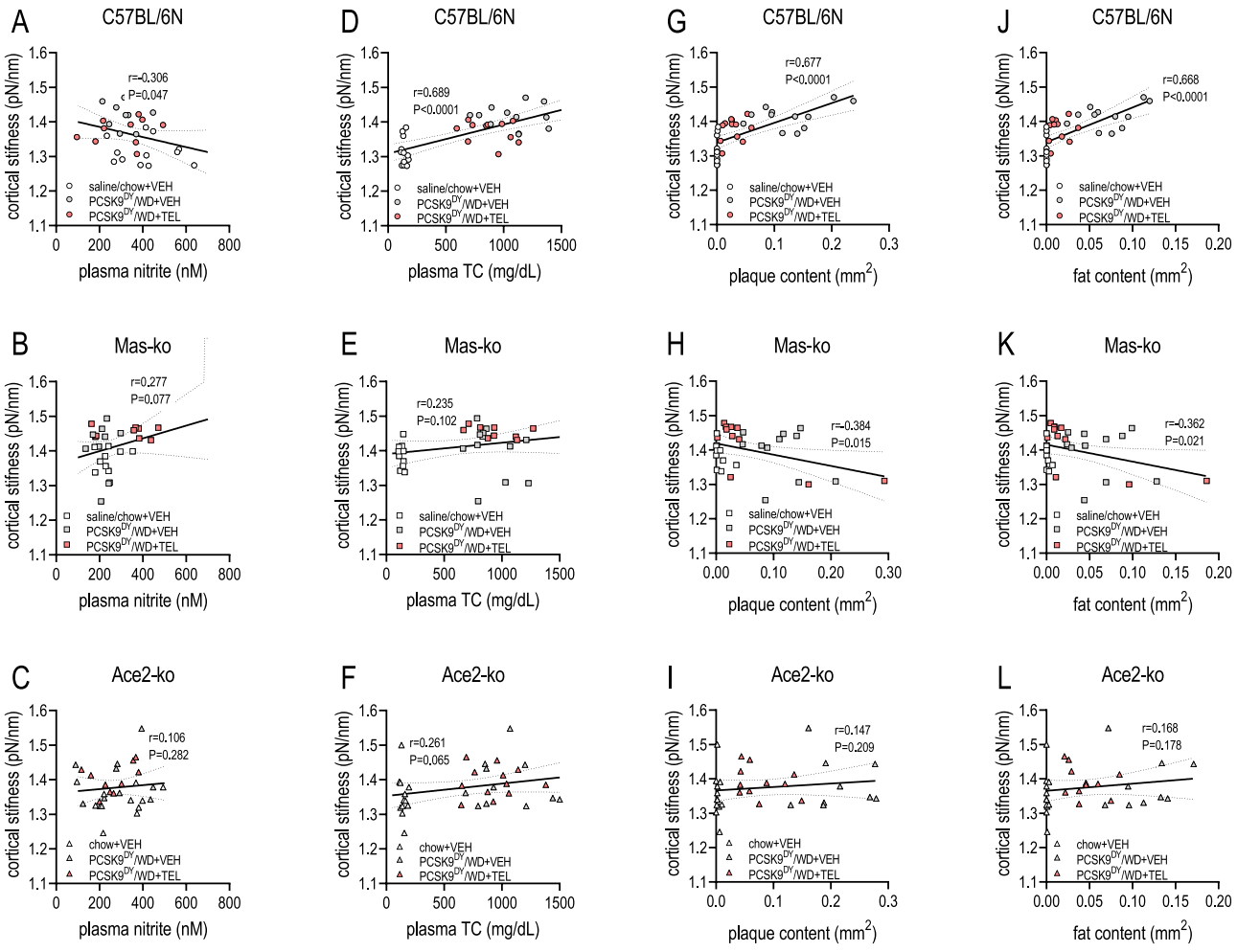

Fig. 5. Pearson correlation analyses between cortical stiffness and plasma levels of nitrites or TC or aortic plaque or fat content.

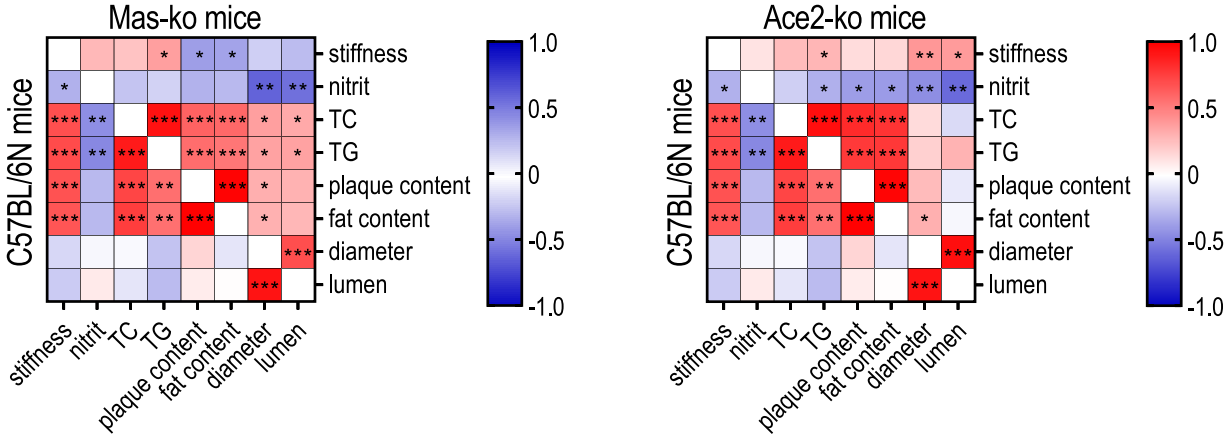

Fig. 6. Summarized presentation of the correlation analyses between various parameters in Mas-ko and Ace2-ko compared to the C57BL/6 N mice which were treated with saline/chow+VEH, PCSK9^{DY}/WD+VEH or PCSK9^{DY}/WD+TEL. Correlation analyses were performed by a one-side Person test.

Furthermore, we have identified 444 genes that were exclusively regulated in C57BL/6 N, but not in Mas-ko and Ace2-ko mice upon PCSK9^{DY}/WD intervention. Among these genes, 130 are associated with atherosclerosis ([66]; Tab. S8). The expression levels of the top 15 and bottom 15 genes out of the 444 genes are shown in Fig. 8Ab, where of these 30 genes only *Myh1, Pvalb, Slc15a1, Trim31, Cyp1a1* are associated with atherosclerosis. In addition, it is interesting that Ren1 was upregulated in the C57BL/6 N but not the Ace2-ko and Mas-ko mice as a result of the PCSK9^{DY}/WD intervention (Tab S8). Conversely, we found 42 genes that were regulated upon PCSK9^{DY}/WD in Mas-ko as well as in Ace2-ko but not in C57BL/6 N mice. Eighteen of these genes are associated with atherosclerosis according to the CTD Gene-Disease Associations dataset [66], including *Dio2, Hk2, S100b, Plin5, Slc24a3, Isyna1* (Fig. 8Ac and Tab. S9).

Next, we addressed the question of how TEL treatment influences gene expression. In C57BL/6 N mice, 35 genes (3/32 up/down) were

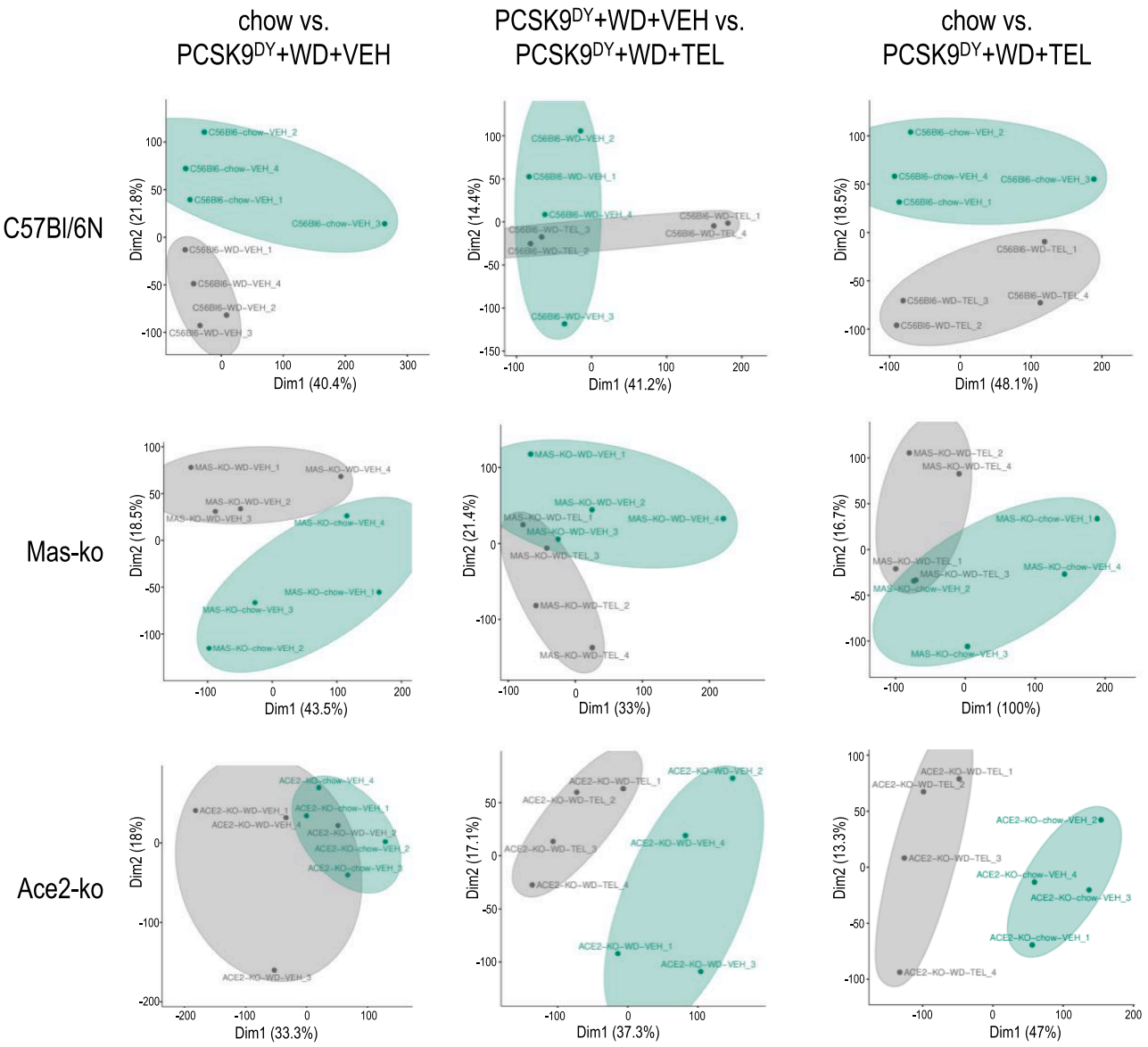

Fig. 7. Principal component analyses (PCA) using FactoMineR to identify the two groups of genes (=dimensions) incorporating the largest amount of divergence. Comparison between chow-controls and upon PCSK9^{DY}/WD treatment and daily TEL or vehicle application in C57BL/6 N, Mas-ko and Ace2-ko mice.

differently expressed between the TEL or vehicle-treated PCSK9^{DY}/WD positive mice (Fig. S11). 16 of these 35 genes are associated with atherosclerosis (Tab S10). Moreover, 15 of these 35 genes were almost counter-regulated by TEL to the same extent as the gene upregulation in response to the PCSK9^{DY}/WD intervention where again 9 of these genes are associated with atherosclerosis, including *Myh1, Pvalb, Ckm, Tnntl3, Mmp12, Acta1, Npr3* and *Fam20c* (Fig. 8B).

Gene expression of the different RAAS components differed not between chow-fed C57BL6/N and transgenic mice, with the exception of a slightly lower AT2 expression in ACE2-Mas ko mice compared to wild-type controls (Fig. S13). In wt controls, an approx. 10-fold increase in *Ace2* expression is noticeable upon PCSK9^{DY}/WD-intervention, which is at least partially reduced by TEL. Such an influence on *Ace2* expression is not observed in each transgenic line. Except of AngI expression, neither PCSK9^{DY}/WD intervention nor TEL treatment had any influence in any mouse line on Mas. An increased expression of *Ren1*, *ACE* and *Agtr1a* after TEL therapy was noticeable in the ACE2-ko mice (Fig. S14). This suggests that structural and functional improvements resulting from TEL treatment cannot quite be associated with the regulation of AT1 and Mas receptors or the enzymes involved in angiotensin biosynthesis. Adressing gene regulation within the NO pathway, we found upregulation in dependence of PCSK9^{DY}/WD intervention and a corresponding downregulation by TEL of Nos1 in C57BL/6 mice, but not in the transgenic lines (Fig. S15).

In contrast to the C57BL/6 N strain, more genes (2424 in total: 1165 up vs 1259 down) were differentially expressed in the Ace2-ko mice in response to TEL treatment compared to the VEH-treated mice. Comparing these 2424 genes with the 652 genes that were regulated in Ace2-ko mice by the PCSK9^{DY}/WD intervention compared to the chow controls, an intersection of 274 genes was identified. Although significant, most of these genes were only slightly altered. Most of these genes were also regulated in the same way. Twenty-three of these 274 genes were counter-regulated by TEL in the Ace2-ko mice. However, only 8 of these genes are associated with atherosclerosis (*Igkv12–98, Hsd17b6, Mep1b, Npc1l1, Hdac11, Rbl1, Fam20c, Abcg1*) and this association was also rather weak according to the database [66] (Tab S11).

In Mas-ko mice, treatment with TEL significantly altered gene expression of 12 genes compared to the VEH-treated PCSK9^{DY}/WD animals where eight of these 12 genes are regulated by TEL in opposition to PCSK9^{DY}/WD intervention under VEH treatment and 6 of these 8 genes

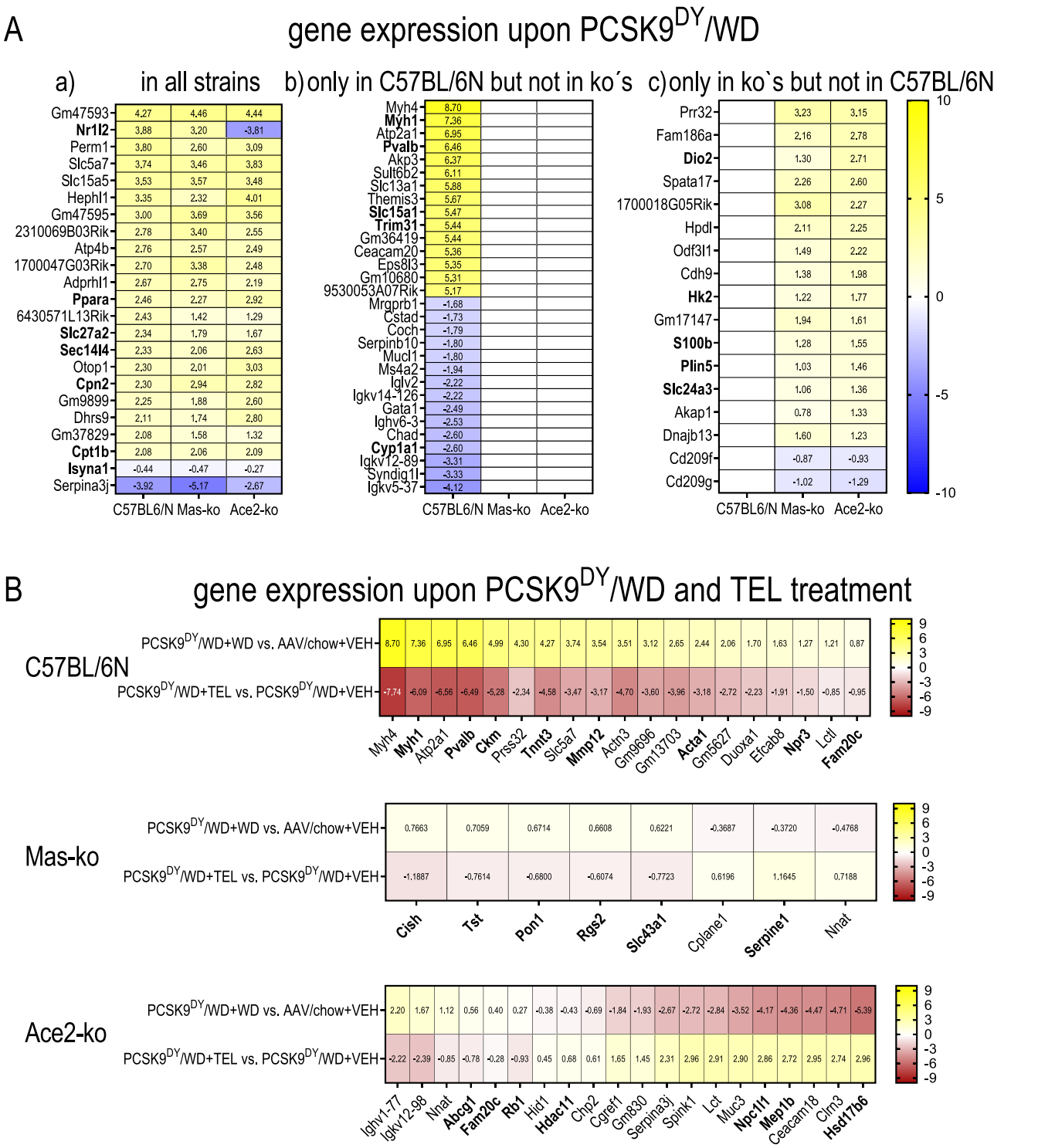

Fig. 8. Differential gene expression (log2fc) in abdominal aorta segments of C57BL/6 N, Mas-ko or Ace2-ko mice. Fig. A shows prominent changes upon PCSK9^{DY}/WD intervention compared to saline/chow treatment of genes which were observed in all 3 mouse lines (a) or which were only observed in C57BL/6 N but not in the two ko lines (b) or which were selectively not expressed in the C57BL/6 N controls but in Mas-ko and Ace2-ko mice (c). Fig. B shows changes in gene expression in the different mouse strains, which were altered by the PCSK9^{DY}/WD intervention, but were also counter-regulated by the TEL therapy. The genes associated with atherosclerosis are highlighted in bold (according to [66]).

are associated with atherosclerosis [66] (Fig. 8B, Tab S12).

Upon KEGG pathway analyses, the insulin resistance and PPARγ signaling pathway were upregulated in all 3 mouse strains after PCSK9^{DY}/WD- compared to chow/VEH-treatment (Fig. S12). The concordance between the upregulated KEGG pathways was higher between the C57BL/6 N and Mas-ko mice (6/9) than between the C57BL/6 N and Ace2-ko mice (3/9) (Fig. S12). The consistency in the downregulated pathways was low in the 3 different mouse strains. (Fig. S12). The lower expression of the RAAS pathway in the chow-fed Mas-ko mice compared to the PCSK9^{DY}/WD intervention was striking.

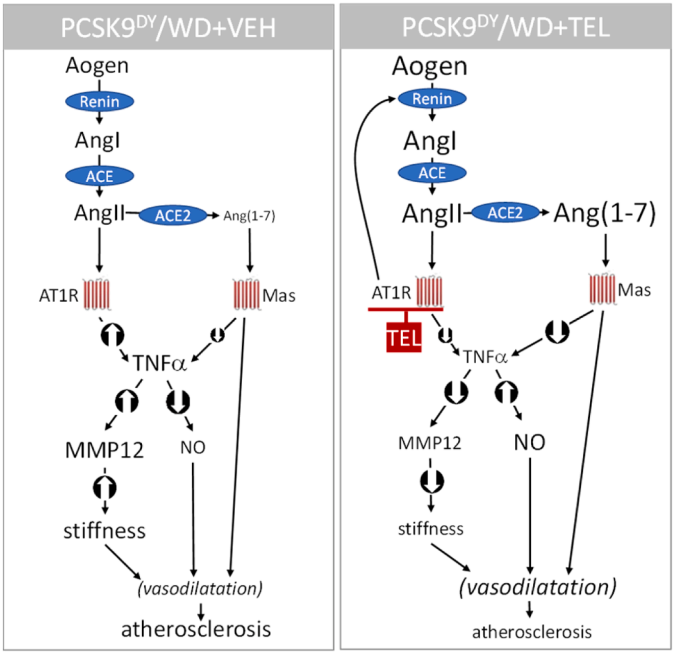

Fig. 9. Graphical abstract indicating that a TNFα-dependent mechanism upregulates expression of MMP12 and NO, thus contributing to increase in cortical stiffness. It is further concluded that increased cortical stiffness leads to impaired vasodilation and thus promotes the development of atherosclerosis. However, since we did not perform any experiments on vasodilation, this conclusion is in italics to emphasize that it is based more on findings in the literature (see discussion) and less on experimental data. TEL counterregulated these pathways via at least partial stimulation of the ACE2/Ang(1−7)/Mas axis.

3. Discussion

For a discussion of the data on weight regulation and glucose homeostasis, see Suppl Data. As the main finding of this study, we demonstrated that upon TEL, cortical stiffness of the aortic ECs is decreased which was accompanied by an increased bioavailability of NO.

3.1. Strain differences

PCSK9^{DY}/WD-treated C57BL/6 N mice developed hallmarks of atherosclerosis which has already been shown by others [31,32,36,43,52].

Overall, we observed that, compared to C57BL6/N mice, similar TEL-induced changes were observed in the two transgenic mouse lines, particularly with regard to the primary parameters of our study, namely cortical stiffness and plasma NO. The most pronounced difference between the two transgenic mouse lines was observed with regard to a different weight regulation per se but also as a result of TEL treatment. This raises the question of the consequences and differences of ACE2 and Mas knock out with regard to the suppression of the ACE2/Ang(1−7)/Mas axis. One could assume that ACE2/Ang(1−7)/Mas receptor signaling is completely suppressed in Mas-ko mice while the metabolism of Ang II may be partially inhibited in ACE2-ko mice, potentially leading to the enhancement of the ACE/AngII/AT1R axix. However, RNAseq analysis revealed no difference in the gene expression of the different RAAS components, with the exception of a slightly lower AT2 expression in ACE2-Mas ko mice compared to wild-type controls (Fig. S13). Furthermore, it should be noted that even with total Mas deficiency, Ang (1−7) also acts via the Mrgd receptor [67] and thus a complete shutdown of the Ang(1−7) effect is only possible via the Mas/Mrgd double knockout [68]. Even with the ACE2 knockout, complete suppression of Ang(1−7) biosynthesis cannot necessarily be assumed, since angiotensinogen is also degradated to Ang1–12, which could then be metabolized via NEP to Ang(1−7) [67]. Clear differences exist between the two transgenic mouse lines with regard to weight regulation, which, however, can be attributed to a serotonin-dependent mechanism (see also the extended discussion in the Suppl Data).

3.1.1. Atherosclerotic lesions

Pro-inflammatory cytokines such as TNFα or MIP2 increased upon PCSK9^{DY}/WD-intervention in C57/BL/6, but not in transgenic mice. In fact, we have expected even higher cytokine levels in transgenic mice, as Ang(1−7) reveals vascular anti-inflammatory properties [69]. Stimulation of the ACE2/Ang(1−7)Mas axis is claimed to reduce the atherosclerosis risks as 1.), Ang(1−7) diminished macrophage infiltration, MCP-1, IL6, TNFα, NFKβ, vascular cell adhesion protein 1 (VCAM-1), reactive oxygen species (ROS) levels, apoptosis and increased NO release in ApoE ko mice [70,71]; 2.), Ang(1−7) improved ACh-induced relaxation in abdominal aortic sections of ApoE-ko mice [26] and 3.), Mas/ApoE-dko mice and Ace2/ApoE-dko mice showed aggravated signs of local vascular inflammation [27,29]. Thus, the question remains, why were atherogenesis and inflammation not aggrevated in both transgenic compared to C57BL/6 N mice upon the PCSK9^{DY}/WD intervention. Strikingly, the extend of plaque burden in our study was > 3-fold higher than in chow-fed ApoE-ko mice [27], which let us to speculate that aggravation of atherosclerosis in response to ACE2 deficiency is only possible if the extent of atherosclerotic changes per se is not already maximal. This assumption is supported by the head-to-head comparison of both atherosclerotic mouse models, which showed smaller lesion areas in the chow-fed ApoE-ko by more than half as compared to the WD-fed PCSK9^{DY}-treated mice [32]. In the Mas-ko mice also used, cortical stiffness was increased compared to C57BL/6 N, but as a result of PCSK9^{DY}/WD intervention, neither plaque burden nor cortical stiffness were more pronounced than in C57BL/6 N controls, confirming recent findings demonstrating that deletion of Mas in ApoE-ko mice had no effect on concomitant atherosclerosis.[72] However, this conflicts with others showing that chronic Ang(1−7) treatment attenuated the development of atherosclerosis in ApoE-ko but not in ApoE/Mas-ko mice [73] and that a Mas agonist reduces the atherosclerotic burden in ApoE-ko mice, while a Mas antagonist increases it [74]. These discrepancies may again be attributable to differences in atherosclerotic development, as in both cited studies, the extent of atherosclerotic lesions was significantly less severe than in ours. From a mechanistic perspective, Ang(1−7)-induced attenuation of atherosclerosis was attributed to a NO-dependent mechanism [73]. The decrease in the expression of eNOS in ApoE-ko mice and normalization by Ang(1−7) confirmed the NO-dependence postulated [26]. This dependency was also found in our study, as plasma NO and cortical stiffness correlated negatively in the C57BL/6 N mice but even positively in the Mas-ko and also Ace2-ko mice. In Mas-ko mice, NO was reduced to 50 %, which is in accordance to previous observations [75] and also consistent with the finding that Mas receptor activation contributes to NO bioavailability [76]. Thus, it is convincing that cortical stiffness is higher and that the NO bioavailabilty tends to correlate positively with cortical stiffness in chow-fed Mas deficient mice, but negatively in C57BL/6 N mice.

3.1.2. Vascular dysfunction

In confirmation of our previous study [36], the mechanical stiffness of the endothelial cortex was enhanced upon PCSK9^{DY}/WD-treatment in C57BL/6 N mice, which was attributed., to an insertion and/or activity of specific membrane proteins, e.g. ENaC (epithelial Na^+ channel), ion composition of the extracellular fluid and the polymerization state of the cortical actin [57,77–79]. Such a stiffening was not observed in Mas-ko and Ace2-ko mice, even though plaque burden and plasma lipids were increased. This suggests that histological vascular examinations may not necessarily be sufficient to characterize atherosclerosis, but should rather be strengthened by functional results. However, this conclusion may be quite daring as the endothelial stiffness and the atherosclerotic

plaque load or the plasma cholesterol levels correlated positively in different atherosclerotic models [80–82] including the PCSK9^{DY}/W-D-induced model [36]. Since stiffness per se was already increased in the Mas-ko and also in the Ace2-ko mice, one could speculate whether this higher stiffness in the transgenic mice is almost maximal and therefore not further increasable by PCSK9^{DY}/WD. This could be due to the fact that there is also a limit related to the degree of polymerization of the actin and the linker proteins. AFM-technique also allowed to investigate properties of endothelial glycocalyx (EG). The EG is a negatively charged, brush-like multifunctional layer of membrane-bound, carbohydrate-rich molecules, mostly consisting of glycoproteins and proteoglycans. Hyaluronan (HA), a glycosaminoglycan, is an important constituent of the EG that regulates inflammation and repair. By providing a direct link to the interior of the cell, HA contributes to maintaining glycocalyx integrity; emerging evidence indicates a close association between EG deterioration, concomitant loss of HA and the onset of endothelial dysfunction, a phenomenon that is involved in atherosclerosis dyslipidemia [83–86]. In contrast to cortical stiffness, neither the mechanical properties of the EG nor the height was altered by the PCSK9^{DY}/WD intervention, by TEL therapy, nor in the different mouse lines. The consequence of increased cortical stiffness is functionally detrimental as the relationship between endothelial stiffness, arterial stiffness and the development of hypertension appears to be a chicken-and-egg dilemma [87–89]. Even though we did not measure blood pressure in our study due to methological limitations, the increased cortical stiffness and decreased plasma NO levels could be associated with the increased blood pressure in Mas-ko mice which has been described elsewhere [90–92]. In Ace2-ko mice, various reports suggested elevated blood pressure when using the sensitive telemetric approach [27,90,93]. These results indicate endothelial dysfunction which is further confirmed by the observation that dilatation to acetylcholine was lower in the basilar artery from Ace2-ko than in wild type mice [94]. Accordingly, cortical stiffness tended to be higher in Ace2-ko mice compared to C57BL/6 N controls. Also addressing the question whether genetic deletion of Ace2 induces vascular dysfunction, Rabelo et al. show in 20–22 week-old male Ace2-ko compared to C57BL/6 N mice (which is comparable to our setting) that the blood pressure is higher while aortic eNOS expression and eNOS acivity is lower and NO plasma concentration is reduced [95]. We observed a tendency ($p = 0.142$) that plasma nitrite levels were decreased in the Ace2-ko animals in this study.

3.1.3. Gene regulation

KEGG analyses of PCSK9^{DY}/WD treated C57BL/6 N mice annotate the differentially expressed genes to an upregulation of insulin resistance, metabolic, starch sucrose metabolism, and fat digestion and absorption pathways. In a study conducted in parallel with this one [52], we particularly found by KEGG analyses an upregulation of inflammatory pathways in thoracic segments of aortas of PCSK9^{DY}/WD C57BL/6 N mice. It is assumed that these differences may be attributed to different patterns of atherosclerotic remodeling in the thoracic and abdominal aorta [96]. To identify specific gene expression in different mouse strains upon PCSK9^{DY}/WD intervention, we pursued 3 different approaches: to identify first, which genes were equally regulated in all mouse lines; second, which genes were exclusively expressed in C57BL/6 N mice and thirdly, which genes were exclusively expressed in Ace2-ko as well as in Mas-ko mice. The first search strategy revealed a total of 101 genes (including *Cpt1b, Nr1i2, Ppara, Cpn2*), the second aspect 130 genes (including *Myh1, Palvb, Trim31, Slc15a1* and *Cyp1a1*) and the third 18 genes (including *Dio2, Hk2, S100b, Plin5, Slc24a3* and *Isyna1*), which were either regulated in all strains or selectively in the CB57BL/6 N or the two trasgenic lines depending on the atherosclerotic changes. For a more detailed discussion of the (functional) significance of these genes, particularly in the light of atherosclerosis, and whether these genes interact with the RAAS please refer to the discussion in the supplementary data for reasons of clarity.

3.2. TEL treatment

In 2000, an editorial highlighted the anti-atherosclerotic potential of ARBs [97], and since then the anti-atherosclerotic efficacy even of TEL was well established in experimental studies using different atherosclerosis models [98–102] and also in clinical trials [103]. Numerous studies were carried out to identify the underlying mechanism. In this respect, the anti-atherosclerotic efficacy of TEL was attributed to multiple mechanisms such as, a) a suppression in superoxide production [104], b) an induction of autophagy [105]; c) an increase of the permeability of endothelial cells through zonula occludens-1 [106]; d) an inhibition of the pro-inflammatory β2-integrin MAC-1 expression in lymphocytes [107]; e) an AMPK activation thus inhibiting basal and PDGF-stimulated VSMC proliferation [108], f) an increase of NO bioavailability [109] and g) a modulation of the gastrointestinal microbiota [110,111]. In addition, there seems to be disagreement as to whether or not the TEL-induced anti-atherogenic effect is dependent on its PPARγ pleiotropic potency, as typical PPARγ agonists attenuates aortic stiffening in obesity [112]. At least some studies indicate such a dependence for ARBs [102,109,113] others do not [114] and still others show at least a partially dependent effect [115].

In accordance with the afore mentioned studies, we here confirmed in the PCSK9^{DY}/WD-induced atherosclerosis model, that the expression of atherosclerotic lesions and plasma levels of lipids were clearly decreased with TEL treatment. Moreover, TEL normalized TNFα or MIP2 plasma levels, indicating anti-inflammatory potency, which was however not observed in patients suffering from atherosclerosis [116]. The genes of most interest that were found to be counter-regulated upon TEL compared to the PCSK9^{DY}/WD C57BL/6 N controls include *Myh1, Pvalb, Ckm, Tnntl3, Mmp12, Acta1, Npr3* and *Fam20c*, as these genes are all associated with atherosclerosis. Of these listed genes, Mmp12 appears to be the most interesting, as MMP12 was identified in a large scale proteomic human trial as a potential novel circulating biomarker for aortic stenosis risk [117,118]. *Mmp12* is crucial to the initiation and progression of atherosclerosis via degradation of the elastic layers and/or basement membrane [119] thereby influencing arterial stiffening [120]. The TEL-dependent down-regulation of *Mmp12* as shown here and elsewhere [121] appears conclusive because AngII itself has increased the Mmp12 gene expression in VSMCs [122] and mouse aorta [123–125]. As the TEL-dependent downregulation of MMP12 was no longer detectable in Mas-ko and Ace2-ko mice, a dependency on ACE2/Ang(1−7)/Mas axis is supposed, which supports findings showing that Ang(1−7) blocks Mmp12 expression [126–128]. From a mechanistic point of view, it furthermore seems interesting that Mmp12 expression is TNFα-dependent [129] and that Tnfa expression itself is upregulated by AngII and downregulated by Ang(1−7) [130]. The drug-relevant significance of a downregulation of *Mmp12* is also emphasized because statins as typical anti-atherosclerotic drugs markedly lower Mmp12 expression [131]. As MMP12 is crucial for influencing arterial stiffening [120] and we here demonstrated prevention of stiffening in C57BL/6 N mice upon TEL-treatment we have obtained evidence that TEL-induced improvements/changes at structural and biochemical level also have a functional consequence in atherosclerosis. In this functional context, ARBs were previously shown to prevent arterial stiffness in elderly patients with hypertension [132]. In particular, the lack of correlation between plaque load and stiffness in the Mas-ko and Ace2-ko mice suggests that this functional property is dependent on the ACE2/Ang(1−7)/Mas axis. A detailed description of the other mentioned genes in the context with components of the RAAS, NO or eNOS expression, TNFα or arterial stiffness is refrained here and reference is made to the supplementary data, especially as hardly any literature was identified on the basis of the a pubmed search. It could only be shown that Acta1 expression in cardiomyocytes is increased by AngII [133].

As claimed above, ARBs enhanced NO bioavailability thus contributing to its benefitial effects in treatment of atherosclerosis [109]. Such a

mechanism is supported by our study as we found the negative correlation in C57BL/6 N mice but not anymore in both transgenic strains. To address the concern that determination of plasma NO is no sufficient evidence, we have compiled the RNAseq data for the NO pathway with mainly being NOS1 upregulated in dependence of $PCSK9^{DY}$/WD intervention and a corresponding downregulated by TEL of Nos1 in C57BL/6 mice, but not in the transgenic lines. Such an upregulation of Nos1 expression has also been shown in human atherosclerosis and was interpreted as a quasi counterregulation to a decrease in Nos3. However, we could not observe any regulation of Nos3 expression, which would be consistent with the idea that the Nos3 regulation in atherosclerosis is a posttranslational regulation [134]. However, due to limited sample material, we were unable to perform further blot analysis to show such a regulation at the protein level. Our findings of increased TEL-induced NO levels in C57BL6/N mice are also consistent with older reports that also reported increased nitric oxide bioavailability and atherosclerotic change [109] and also that telmisartan activates endothelial nitric oxide synthase in vascular endothelial cells TEL activates endothelial nitric oxide synthase in vascular endothelial cells [135] and that TEL-pretreatment decreased LPS-induced expression of iNOS in a macrophage cell line [102]. Ikejima attributed the ARBs-dependend enhanced NO bioavailability to a PPARγ mediated mechanism [109]. However, an TNFα-mediated effect may also be involved as TNFα blocks eNOS expression in endothelial cells therby reduced NO bioavailability [136,137]. Accordingly, TNFα expression is enhanced in atherosclerotic mice C57BL/6 N mice as shown here and elsewhere [52] and was normalized by TEL.

We finally sought to answer the question of whether the anti-atherosclerotic effect of TEL is diminished in mice with ACE2 or Mas deficiency because Ang(1−7) has opposing cardiovascular and metabolic effects to AngII [138] and ARB-induced effects that may also be attributed to an ACE2/Ang(1−7)/Mas axis-dependent mechanism [15]. Considering the findings that Ang(1−7) reduced atherosclerosis plaque load but improved vasorelaxation via Mas receptor activation in the ApoE-ko model [24,74], we expected the TEL-induced improvement in the two transgenic mouse models to be at least partially abolished. The correlation analyses clearly suggest, at least at the functional level, that the increased cortical stiffness in the C57BL/6 N controls, which is negatively associated with plasma NO but positively associated with plaque burden and TC plasma concentration, is no longer evident in the Mas-ko or Ace2-ko mice, as in both transgenic mouse lines the correlations observed in the C57BL/6 N mice were abolished or even reversed. This suggest that on functional levels the anti-atherosclerotic effect of TEL can be attributed to an ACE2/Ang(1−7)/Mas axis-dependent mechanism. However, it is unclear why cortical stiffness was not reduced by TEL in the transgenic lines, but plaque burden was. Strikingly, the plasma levels of TC and some cytokines (e.g. TNFα, MIP2, MCP1/CCL2, IL12p70, KC, IL10) were not reduced by TEL in the transgenic lines as in the C57BL/6 N controls, but even increased.

In summary (see graphical abstract), it is concluded that under VEH treatment and $PCSK9^{DY}$/WD intervention, AT1 receptor mediated TNFapha expression is increased with consecutive upregulation of *Mmp12*, which in turn leads to increased endothelial stiffness. This contributes to a worsening of vasodilation in the atherosclerotic model, as does the reduced TNFα-dependent NO bioavailability. Treatment with TEL not only blocks the AT_1R-mediated signaling pathway but also leads to an increase in Ang(1−7). Using Mas-ko and Ace2-ko mice, we were able to show that activation of Mas, on the one hand, reduces TNFα expression, which leads to lower Mmp12 expression and endothelial stiffness as well as increased NO bioavailability. These indirect effects, like the direct effect, contribute to vasodilation. Thus, it could also be confirmed for atherosclerosis that the beneficial effects of ARBs are not only based on the blockade of the ACE/AngII/AT_1R axis but also on stimulation of the ACE2/Ang(1−7)/Mas axis. However, it should be noted that the conclusion regarding a change in dilation (not possible due to lack of sample material) or blood pressure regulation (not possible due to the impracticability of such a measurement) is speculative and cannot be supported by data from this study. Findings from the literature do, however, address the correlation between blood pressure and cortical stiffness [139]. A second limitation is that, as in our previous studies in which we examined the effects of the RAAS on body weight and atherosclerosis in rodents, we only included male animals to minimize the variability of the results [1–3,5–11,15,51,52]. The challenge for the planned future study is to also examine a possible gender difference.

Author contribution

L.A, T.K., B.F, F.R., M.L., F.S., I.S., S.H., W.H., T.R., Z.A. S.H. O.J.M., U.M., N.A., C.V. and M.B performed the experiments; R.B., Z.A., K.K-V. and W.R. designed study and protocols; L.A, T.K., Z.A., B.F., T.R., F.R., C. K., K.K-V and W.R. analyzed data, and L.A, T.K., and W.R. wrote the manuscript. All authors made substantial contributions in the preparation of the manuscript

Funding

This work was supported by two research grants (81X2700128 and 81X2700138) from the German Centre for Cardiovascular Research (DZHK), by grants from the Deutsche Forschungsgemeinschaft (KU 1496/7–1, KU 1496/7–3, INST 392/141–1 FUGG) and by a research grant from the German Research Foundation to the GRK 1957 “Adipocyte-Brain Crosstalk”, University of Lübeck.

CRediT authorship contribution statement

Kuenne Carsten: Writing – review & editing, Methodology, Investigation, Formal analysis, Data curation. **Klersy Tobias:** Writing – original draft, Visualization, Validation, Methodology, Investigation, Formal analysis, Data curation. **Vahldieck Carl:** Writing – review & editing, Methodology, Investigation. **Achner Leonie:** Writing – original draft, Visualization, Validation, Methodology, Investigation, Formal analysis, Data curation. **Aherrahrou Zouhair:** Writing – review & editing, Methodology, Investigation, Formal analysis. **Häuser Walter:** Writing – review & editing, Methodology. **Reinberger Tobias:** Writing – review & editing, Methodology, Investigation, Formal analysis. **Spiecker Frauke:** Writing – review & editing, Methodology. **Müller Oliver J.:** Writing – review & editing, Resources, Methodology, Conceptualization. **Stölting Ines:** Writing – review & editing, Methodology. **Kusche-Vihrog Kristina:** Writing – review & editing, Resources, Methodology, Investigation, Funding acquisition, Conceptualization. **Lopez Melina:** Writing – review & editing, Methodology, Investigation, Formal analysis, Data curation. **Bader Michael:** Writing – review & editing, Resources, Methodology, Conceptualization. **Brandes Ralf P.:** Writing – review & editing, Resources, Methodology, Investigation, Funding acquisition, Conceptualization. **Alenina Natalia:** Writing – review & editing, Methodology. **Matschl Urte:** Writing – review & editing, Methodology. **Fels Benedikt:** Writing – review & editing, Methodology, Investigation, Formal analysis. **Rezende Flavia:** Writing – review & editing, Methodology, Investigation, Formal analysis, Data curation. **Hille Susanne:** Writing – review & editing, Methodology. **Raasch Walter:** Writing – original draft, Visualization, Validation, Supervision, Resources, Project administration, Methodology, Investigation, Funding acquisition, Formal analysis, Data curation, Conceptualization.

Declaration of Competing Interest

All authors declare no conflicts of interest.

Acknowledgments

The authors thank Urszula Frackowski, Annett Liebers and Petra Bruse for excellent technical support. The authors gratefully acknowledge Sherryl Sundell for improving the English style. Parts of the work covered in the article were presented at the 7rd Pharm-Tox Summit DIGITAL Germany, 2022 (Naunyn-Schmiedebergs Archives of Pharmacology, 395 (Suppl. 1, S55 [25])

Informed consent

Not necessary: the results of this study are based on animal studies that were approved by the appropriate state authority (see Methods section) and not on human studies. Therefore, it was not necessary to obtain informed consent.

Appendix A. Supporting information

Supplementary data associated with this article can be found in the online version at doi:10.1016/j.biopha.2025.117990.

Data availability

The data that support the findings of this study are available from the corresponding author upon reasonable request. Some data may not be made available because of privacy or ethical restrictions.

References

[1] A. Miesel, H. Muller-Fielitz, O. Johren, F.M. Vogt, W. Raasch, Double blockade of angiotensin II (AT(1))-receptors and ACE does not improve weight gain and glucose homeostasis better than single-drug treatments in obese rats, Br. J. Pharm. 165 (8) (2012) 2721–2735.

[2] H. Muller-Fielitz, J. Landolt, M. Heidbreder, S. Werth, F.M. Vogt, O. Johren, W. Raasch, Improved insulin sensitivity after long-term treatment with AT1 blockers is not associated with PPARgamma target gene regulation, Endocrinology 153 (3) (2012) 1103–1115.

[3] H. Muller-Fielitz, N. Hubel, M. Mildner, F.M. Vogt, J. Barkhausen, W. Raasch, Chronic blockade of angiotensin AT(1) receptors improves cardinal symptoms of metabolic syndrome in diet-induced obesity in rats, Br. J. Pharm. 171 (3) (2014) 746–760.

[4] H. Muller-Fielitz, A. Markert, C. Wittmershaus, F. Pahlke, O. Johren, W. Raasch, Weight loss and hypophagia after high-dose AT1-blockade is only observed after high dosing and depends on regular leptin signalling but not blood pressure, Naunyn Schmiede Arch. Pharm. 383 (4) (2011) 373–384.

[5] H. Muller-Fielitz, M. Lau, C. Geissler, L. Werner, M. Winkler, W. Raasch, Preventing leptin resistance by blocking angiotensin II AT1 receptors in diet-induced obese rats, Br. J. Pharm. 172 (3) (2015) 857–868.

[6] F. Schuster, G. Huber, I. Stolting, E.E. Wing, K. Saar, N. Hubner, W.A. Banks, W. Raasch, Telmisartan prevents diet-induced obesity and preserves leptin transport across the blood-brain barrier in high-fat diet-fed mice, Pflug. Arch. 470 (11) (2018) 1673–1689.

[7] G. Huber, M. Ogrodnik, J. Wenzel, I. Stölting, L. Huber, O. Will, E. Peschke, U. Matschl, J.B. Hövener, M. Schwaninger, D. Jurk, W. Raasch, Telmisartan prevents high-fat diet-induced neurovascular impairments and reduces anxiety-like behavior, J. Cereb. Blood Flow. Metab.: Off. J. Int. Soc. Cereb. Blood Flow. Metab. (2021), 271678x211003497.

[8] E. Rawish, L. Nickel, F. Schuster, I. Stölting, A. Frydrychowicz, K. Saar, N. Hübner, A. Othman, L. Kuerschner, W. Raasch, Telmisartan prevents development of obesity and normalizes hypothalamic lipid droplets, J. Endocrinol. 244 (1) (2020) 95–110.

[9] M. Winkler, J. Schuchard, I. Stolting, F.M. Vogt, J. Barkhausen, C. Thorns, M. Bader, W. Raasch, The brain renin-angiotensin system plays a crucial role in regulating body weight in diet-induced obesity in rats, Br. J. Pharm. 173 (10) (2016) 1602–1617.

[10] L. Beckmann, A. Künstner, M.L. Freschi, G. Huber, I. Stölting, S.M. Ibrahim, M. Hirose, M. Freitag, E.A. Langan, U. Matschl, C.E. Galuska, B. Fuchs, J. K. Knobloch, H. Busch, W. Raasch, Telmisartan induces a specific gut microbiota signature which may mediate its antiobesity effect, Pharmacol. Res. 170 (2021) 105724.

[11] L. Nickel, A. Sünderhauf, E. Rawish, I. Stölting, S. Derer, C. Thorns, U. Matschl, A. Othman, C. Sina, W. Raasch, The AT1 receptor blocker telmisartan reduces intestinal mucus thickness in obese mice, Front Pharm. 13 (2022) 815353.

[12] S.H. Santos, L.R. Fernandes, E.G. Mario, A.V. Ferreira, L.C. Porto, J.I. Alvarez-Leite, L.M. Botion, M. Bader, N. Alenina, R.A. Santos, Mas deficiency in FVB/N mice produces marked changes in lipid and glycemic metabolism, Diabetes 57 (2) (2008) 340–347.

[13] K. Blanke, F. Schlegel, W. Raasch, M. Bader, I. Dahnert, S. Dhein, A. Salameh, Effect of angiotensin(1-7) on heart function in an experimental rat model of obesity, Front. Physiol. 6 (2015) 392.

[14] S.H. Santos, J.F. Braga, E.G. Mario, L.C. Porto, M.G. Rodrigues-Machado, A. Murari, L.M. Botion, N. Alenina, M. Bader, R.A. Santos, Improved lipid and glucose metabolism in transgenic rats with increased circulating angiotensin-(1-7), Arterioscler. Thromb. Vasc. Biol. 30 (5) (2010) 953–961.

[15] J. Schuchard, M. Winkler, I. Stolting, F. Schuster, F.M. Vogt, J. Barkhausen, C. Thorns, R.A. Santos, M. Bader, W. Raasch, Lack of weight gain after angiotensin AT1 receptor blockade in diet-induced obesity is partly mediated by an angiotensin-(1-7)/Mas-dependent pathway, Br. J. Pharm. 172 (15) (2015) 3764–3778.

[16] J.M. Andrade, F.O. Lemos, P.S. da Fonseca, R.D. Millan, F.B. de Sousa, A. L. Guimaraes, M. Qureshi, J.D. Feltenberger, A.M. de Paula, J.T. Neto, M. T. Lopes, H.M. Andrade, R.A. Santos, S.H. Santos, Proteomic white adipose tissue analysis of obese mice fed with a high-fat diet and treated with oral angiotensin-(1-7), Peptides 60 (2014) 56–62.

[17] J.M. Oliveira Andrade, A.F. Paraiso, Z.M. Garcia, A.V. Ferreira, R.D. Sinisterra, F. B. Sousa, A.L. Guimaraes, A.M. de Paula, M.J. Campagnole-Santos, R.A. dos Santos, S.H. Santos, Cross talk between angiotensin-(1-7)/Mas axis and sirtuins in adipose tissue and metabolism of high-fat feed mice, Peptides 55 (2014) 158–165.

[18] V.W. Gustaityte, M. Stölting, I. Raasch, W, Influence of AT1 blockers on obesity and stress induced eating of cafeteria diet, J. Endocrinol. 240 (1) (2019) 65–79.

[19] M. Pellegrin, J. Szostak, K. Bouzourene, J.F. Aubert, A. Berthelot, J. Nussberger, P. Laurant, L. Mazzolai, Running exercise and angiotensin ii type i receptor blocker telmisartan are equally effective in preventing angiotensin ii-mediated vulnerable atherosclerotic lesions, J. Cardiovasc. Pharmacol. Ther. 22 (2) (2017) 159–168.

[20] T. Sasaki, M. Kuzuya, K. Nakamura, X.W. Cheng, T. Hayashi, H. Song, L. Hu, K. Okumura, T. Murohara, A. Iguchi, K. Sato, AT1 blockade attenuates atherosclerotic plaque destabilization accompanied by the suppression of cathepsin S activity in apoE-deficient mice, Atherosclerosis 210 (2) (2010) 430–437.

[21] A. Warnholtz, M.A. Ostad, T. Heitzer, F. Thuneke, M. Frohlich, P. Tschentscher, E. Schwedhelm, R. Boger, T. Meinertz, T. Munzel, AT1-receptor blockade with irbesartan improves peripheral but not coronary endothelial dysfunction in patients with stable coronary artery disease, Atherosclerosis 194 (2) (2007) 439–445.

[22] F.P. de Souza-Neto, M. Carvalho Santuchi, E.S.M. de Morais, M.J. Campagnole-Santos, R.F. da Silva, Angiotensin-(1-7) and alamandine on experimental models of hypertension and atherosclerosis, Curr. Hypertens. Rep. 20 (2) (2018) 17.

[23] J. Stegbauer, S.E. Thatcher, G. Yang, K. Bottermann, L.C. Rump, A. Daugherty, L. A. Cassis, Mas receptor deficiency augments angiotensin II-induced atherosclerosis and aortic aneurysm ruptures in hypercholesterolemic male mice, J. Vasc. Surg. (2019).

[24] G. Yang, G. Istas, S. Hoges, M. Yakoub, U. Hendgen-Cotta, T. Rassaf, A. Rodriguez-Mateos, L. Hering, M. Grandoch, E. Mergia, L.C. Rump, J. Stegbauer, Angiotensin-(1-7)-induced Mas receptor activation attenuates atherosclerosis through a nitric oxide-dependent mechanism in apolipoproteinE-KO mice, Pflug. Arch. 470 (4) (2018) 661–667.

[25] N. Toda, K. Ayajiki, T. Okamura, Interaction of endothelial nitric oxide and angiotensin in the circulation, Pharmacol. Rev. 59 (1) (2007) 54–87.

[26] S. Tesanovic, A. Vinh, T.A. Gaspari, D. Casley, R.E. Widdop, Vasoprotective and atheroprotective effects of angiotensin (1-7) in apolipoprotein E-deficient mice, Arterioscler. Thromb. Vasc. Biol. 30 (8) (2010) 1606–1613.

[27] M.C. Thomas, R.J. Pickering, D. Tsorotes, A. Koitka, K. Sheehy, S. Bernardi, B. Toffoli, T.P. Nguyen-Huu, G.A. Head, Y. Fu, J. Chin-Dusting, M.E. Cooper, C. Tikellis, Genetic Ace2 deficiency accentuates vascular inflammation and atherosclerosis in the ApoE knockout mouse, Circ. Res. 107 (7) (2010) 888–897.

[28] B. Dong, C. Zhang, J.B. Feng, Y.X. Zhao, S.Y. Li, Y.P. Yang, Q.L. Dong, B.P. Deng, L. Zhu, Q.T. Yu, C.X. Liu, B. Liu, C.M. Pan, H.D. Song, M.X. Zhang, Y. Zhang, Overexpression of ACE2 enhances plaque stability in a rabbit model of atherosclerosis, Arterioscler., Thromb., Vasc. Biol. 28 (7) (2008) 1270–1276.

[29] A. Hammer, G. Yang, J. Friedrich, A. Kovacs, D.H. Lee, K. Grave, S. Jorg, N. Alenina, J. Grosch, J. Winkler, R. Gold, M. Bader, A. Manzel, L.C. Rump, D. N. Muller, R.A. Linker, J. Stegbauer, Role of the receptor Mas in macrophage-mediated inflammation in vivo, Proc. Natl. Acad. Sci. USA 113 (49) (2016) 14109–14114.

[30] B. Emini Veseli, P. Perrotta, G.R.A. De Meyer, L. Roth, C. Van der Donckt, W. Martinet, G.R.Y. De Meyer, Animal models of atherosclerosis, Eur. J. Pharmacol. 816 (2017) 3–13.

[31] M.M. Bjorklund, A.K. Hollensen, M.K. Hagensen, F. Dagnaes-Hansen, C. Christoffersen, J.G. Mikkelsen, J.F. Bentzon, Induction of atherosclerosis in mice and hamsters without germline genetic engineering, Circ. Res. 114 (11) (2014) 1684–1689.

[32] M. Roche-Molina, D. Sanz-Rosa, F.M. Cruz, J. Garcia-Prieto, S. Lopez, R. Abia, F. J. Muriana, V. Fuster, B. Ibanez, J.A. Bernal, Induction of sustained hypercholesterolemia by single adeno-associated virus-mediated gene transfer of mutant hPCSK9, Arterioscler., Thromb., Vasc. Biol. 35 (1) (2015) 50–59.

[33] K.E. Jarrett, C. Lee, M. De Giorgi, A. Hurley, B.K. Gillard, A.M. Doerfler, A. Li, H. J. Pownall, G. Bao, W.R. Lagor, Somatic editing of ldlr with adeno-associated viral-crispr is an efficient tool for atherosclerosis research, Arterioscler., Thromb., Vasc. Biol. 38 (9) (2018) 1997–2006.

[34] M. Peled, H. Nishi, A. Weinstock, T.J. Barrett, F. Zhou, A. Quezada, E.A. Fisher, A wild-type mouse-based model for the regression of inflammation in atherosclerosis, PloS One 12 (3) (2017) e0173975.

[35] A.E. Vozenilek, C.M.R. Blackburn, R.M. Schilke, S. Chandran, R. Castore, R. L. Klein, M.D. Woolard, AAV8-mediated overexpression of mPCSK9 in liver differs between male and female mice, Atherosclerosis 278 (2018) 66–72.
[36] L. Achner, T. Klersy, B. Fels, T. Reinberger, C.X. Schmidt, N. Groß, S. Hille, O. J. Müller, Z. Aherrahrou, K. Kusche-Vihrog, W. Raasch, AFM-based nanoindentation indicates an impaired cortical stiffness in the AAV-PCSK9(DY) atherosclerosis mouse model, Pflug. Arch. (2022).
[37] Z.C. Cosgun, B. Fels, K. Kusche-Vihrog, Nanomechanics of the endothelial glycocalyx: from structure to function, Am. J. Pathol. 190 (4) (2020) 732–741.
[38] C. Vahldieck, B. Fels, S. Löning, L. Nickel, J. Weil, K. Kusche-Vihrog, Prolonged door-to-balloon time leads to endothelial glycocalyx damage and endothelial dysfunction in patients with st-elevation myocardial infarction, Biomedicines 11 (11) (2023).
[39] B. Fels, A. Beyer, V. Cazaña-Pérez, T. Giraldez, J.F. Navarro-González, D. Alvarez de la Rosa, F. Schaefer, A.K. Bayazit, B. Obrycki, J. Ranchin, U. Holle, K. Querfeld, Kusche-Vihrog, Effects of chronic kidney disease on nanomechanics of the endothelial glycocalyx are mediated by the mineralocorticoid receptor, Int. J. Mol. Sci. 23 (18) (2022).
[40] E. Agabiti-Rosei, M.L. Muiesan, Carotid atherosclerosis, arterial stiffness and stroke events, Adv. Cardiol. 44 (2007) 173–186.
[41] M. Igase, W.B. Strawn, P.E. Gallagher, R.L. Geary, C.M. Ferrario, Angiotensin II AT1 receptors regulate ACE2 and angiotensin-(1-7) expression in the aorta of spontaneously hypertensive rats, Am. J. Physiol. Heart Circ. Physiol. 289 (3) (2005) H1013–H1019.
[42] Y. Ishiyama, P.E. Gallagher, D.B. Averill, E.A. Tallant, K.B. Brosnihan, C. M. Ferrario, Upregulation of angiotensin-converting enzyme 2 after myocardial infarction by blockade of angiotensin II receptors, Hypertension 43 (5) (2004) 970–976.
[43] G.K. Buchmann, C. Schürmann, T. Warwick, M.H. Schulz, M. Spaeth, O.J. Müller, K. Schröder, H. Jo, N. Weissmann, R.P. Brandes, Deletion of NoxO1 limits atherosclerosis development in female mice, Redox Biol. 37 (2020) 101713.
[44] F. Sonntag, K. Köther, K. Schmidt, M. Weghofer, C. Raupp, K. Nieto, A. Kuck, B. Gerlach, B. Böttcher, O.J. Müller, K. Lux, M. Hörer, J.A. Kleinschmidt, The assembly-activating protein promotes capsid assembly of different adeno-associated virus serotypes, J. Virol. 85 (23) (2011) 12686–12697.
[45] A. Jungmann, B. Leuchs, J. Rommelaere, H.A. Katus, O.J. Müller, Protocol for efficient generation and characterization of adeno-associated viral vectors, Hum. gene Ther. Methods 28 (5) (2017) 235–246.
[46] N. Percie du Sert, V. Hurst, A. Ahluwalia, S. Alam, M.T. Avey, M. Baker, W. J. Browne, A. Clark, I.C. Cuthill, U. Dirnagl, M. Emerson, P. Garner, S.T. Holgate, D.W. Howells, N.A. Karp, S.E. Lazic, K. Lidster, C.J. MacCallum, M. Macleod, E. J. Pearl, O.H. Petersen, F. Rawle, P. Reynolds, K. Rooney, E.S. Sena, S. D. Silberberg, T. Steckler, H. Würbel, The ARRIVE guidelines 2.0: updated guidelines for reporting animal research, PLoS Biol. 18 (7) (2020) e3000410.
[47] L. Nickel, A. Sünderhauf, E. Rawish, I. Stölting, S. D, C. Thorns, U. Matschl, C. S, W. Raasch, The AT1 receptor blocker telmisartan reduces intestinal mucus thickness in obese mice, Front Pharm. (2022).
[48] T. Walther, D. Balschun, J.P. Voigt, H. Fink, W. Zuschratter, C. Birchmeier, D. Ganten, M. Bader, Sustained long term potentiation and anxiety in mice lacking the Mas protooncogene, J. Biol. Chem. 273 (19) (1998) 11867–11873.
[49] D. Singer, S.M. Camargo, T. Ramadan, M. Schafer, L. Mariotta, B. Herzog, K. Huggel, D. Wolfer, S. Werner, J.M. Penninger, F. Verrey, Defective intestinal amino acid absorption in Ace2 null mice, Am. J. Physiol. Gastrointest. Liver Physiol. 303 (6) (2012) G686–G695.
[50] M.A. Crackower, R. Sarao, G.Y. Oudit, C. Yagil, I. Kozieradzki, S.E. Scanga, A. J. Oliveira-dos-Santos, J. da Costa, L. Zhang, Y. Pei, J. Scholey, C.M. Ferrario, A. S. Manoukian, M.C. Chappell, P.H. Backx, Y. Yagil, J.M. Penninger, Angiotensin-converting enzyme 2 is an essential regulator of heart function, Nature 417 (6891) (2002) 822–828.
[51] C. Dapper, F. Schuster, I. Stölting, F. Vogt, L.A. Castro e Souza, N. Alenina, M. Bader, W. Raasch, The antiobese effect of AT1 receptor blockade is augmented in mice lacking Mas, Naunyn-Schmiede 'S. Arch. Pharmacol. 392 (7) (2019) 865–877.
[52] L.D. Hernandez Torres, F. Rezende, E. Peschke, O. Will, J.B. Hoevener, F. Spiecker, Ü. Özorhan, J. Lampe, I. Stölting, Z. Aherrahrou, C. Künne, K. Kusche-Vihrog, U. Matschl, S. Hille, R.P. Brandes, M. Schwaninger, O. J. Müller, W. Raasch, Incidence of microvascular dysfunction is increased in hyperlipidemic mice leading to a reduction in cerebral blood flow and an impairment of long-term memory, Front. Endocrinol. 15 (2024).
[53] K. Kusche-Vihrog, K. Urbanova, A. Blanqué, M. Wilhelmi, H. Schillers, K. Kliche, H. Pavenstädt, E. Brand, H. Oberleithner, C-reactive protein makes human endothelium stiff and tight, Hypertens. (Dallas, Tex.: 1979) 57 (2) (2011) 231–237.
[54] V. Drüppel, K. Kusche-Vihrog, C. Grossmann, M. Gekle, B. Kasprzak, E. Brand, H. Pavenstädt, H. Oberleithner, K. Kliche, Long-term application of the aldosterone antagonist spironolactone prevents stiff endothelial cell syndrome, FASEB J.: Off. Publ. Fed. Am. Soc. Exp. Biol. 27 (9) (2013) 3652–3659.
[55] P. Jeggle, C. Callies, A. Tarjus, C. Fassot, J. Fels, H. Oberleithner, F. Jaisser, K. Kusche-Vihrog, Epithelial sodium channel stiffens the vascular endothelium in vitro and in Liddle mice, Hypertens. (Dallas, Tex.: 1979) 61 (5) (2013) 1053–1059.
[56] P. Jeggle, V. Hofschröer, M. Maase, M. Bertog, K. Kusche-Vihrog, Aldosterone synthase knockout mouse as a model for sodium-induced endothelial sodium channel up-regulation in vascular endothelium, FASEB J.: Off. Publ. Fed. Am. Soc. Exp. Biol. 30 (1) (2016) 45–53.
[57] A. Tarjus, M. Maase, P. Jeggle, E. Martinez-Martinez, C. Fassot, L. Loufrani, D. Henrion, P.B.L. Hansen, K. Kusche-Vihrog, F. Jaisser, The endothelial αENaC contributes to vascular endothelial function in vivo, PloS One 12 (9) (2017) e0185319.
[58] R. Aherrahrou, A.E. Kulle, N. Alenina, R. Werner, S. Vens-Cappell, M. Bader, H. Schunkert, J. Erdmann, Z. Aherrahrou, CYP17A1 deficient XY mice display susceptibility to atherosclerosis, altered lipidomic profile and atypical sex development, Sci. Rep. 10 (1) (2020) 8792.
[59] M. Segura-Puimedon, E. Mergia, J. Al-Hasani, R. Aherrahrou, S. Stoelting, F. Kremer, J. Freyer, D. Koesling, J. Erdmann, H. Schunkert, C. de Wit, Z. Aherrahrou, Proatherosclerotic Effect of the alpha1-Subunit of Soluble Guanylyl Cyclase by Promoting Smooth Muscle Phenotypic Switching, Am. J. Pathol. 186 (8) (2016) 2220–2231.
[60] M. Lopez, P.F. Malacarne, A. Gajos-Draus, X. Ding, A. Daiber, J.O. Lundberg, S. Offermanns, R.P. Brandes, F. Rezende, Vascular biotransformation of organic nitrates is independent of cytochrome P450 monooxygenases, Br. J. Pharmacol. 178 (7) (2021) 1495–1506.
[61] A.M. Bolger, M. Lohse, B. Usadel, Trimmomatic: a flexible trimmer for Illumina sequence data, Bioinforma. Oxf. Engl. 30 (15) (2014) 2114–2120.
[62] A. Dobin, C.A. Davis, F. Schlesinger, J. Drenkow, C. Zaleski, S. Jha, P. Batut, M. Chaisson, T.R. Gingeras, STAR: ultrafast universal RNA-seq align, er, Bioinforma. Oxf. Engl 29 (1) (2013) 15–21.
[63] Y. Liao, G.K. Smyth, W. Shi, featureCounts: an efficient general purpose program for assigning sequence reads to genomic features, Bioinforma. Oxf. Engl. 30 (7) (2014) 923–930.
[64] M.I. Love, W. Huber, S. Anders, Moderated estimation of fold change and dispersion for RNA-seq data with DESeq2, Genome Biol. 15 (12) (2014) 550.
[65] CTD Gene-Disease Associations dataset <⟨https://maayanlab.cloud/Harmonizome/gene_set/Atherosclerosis/CTD+Gene-Disease+Associations⟩>).
[66] A.D. Rouillard, G.W. Gundersen, N.F. Fernandez, Z. Wang, C.D. Monteiro, M. G. McDermott, A. Ma'ayan, The harmonizome: a collection of processed datasets gathered to serve and mine knowledge about genes and proteins, Database.: J. Biol. Database. Curation 2016 (2016).
[67] G. Huber, F. Schuster, W. Raasch, Brain renin-angiotensin system in the pathophysiology of cardiovascular diseases, Pharmacol. Res. 125 (Pt A) (2017) 72–90.
[68] A. Tetzner, K. Gebolys, C. Meinert, S. Klein, A. Uhlich, J. Trebicka, Ó. Villacañas, T. Walther, G-protein-coupled receptor MrgD is a receptor for angiotensin-(1-7) involving adenylyl cyclase, cAMP, and phosphokinase A, Hypertension 68 (1) (2016) 185–194.
[69] D.F. Lelis, D.F. Freitas, A.S. Machado, T.S. Crespo, S.H.S. Santos, Angiotensin-(1-7), Adipokines and Inflammation, Metab.: Clin. Exp. 95 (2019) 36–45.
[70] Y. Guang, M. Fanxing, W. Jialin, Z. Yanping, Z. Linlin, Angiotensin-(1-7)/mas axis and vascular inflammation, Eur. Sci. J., ESJ 11 (33) (2015).
[71] Y.H. Zhang, Y.H. Zhang, X.F. Dong, Q.Q. Hao, X.M. Zhou, Q.T. Yu, S.Y. Li, X. Chen, A.F. Tengbeh, B. Dong, Y. Zhang, ACE2 and Ang-(1-7) protect endothelial cell function and prevent early atherosclerosis by inhibiting inflammatory response, Inflamm. Res.: Off. J. Eur. Histamine Res. Soc. 64 (3-4) (2015) 253–260.
[72] A.R. Silva, E.C. Aguilar, J.I. Alvarez-Leite, R.F. da Silva, R.M. Arantes, M. Bader, N. Alenina, G. Pelli, S. Lenglet, K. Galan, F. Montecucco, F. Mach, S.H. Santos, R. A. Santos, Mas receptor deficiency is associated with worsening of lipid profile and severe hepatic steatosis in ApoE-knockout mice, Am. J. Physiol. Regul. Integr. Comp. Physiol. 305 (11) (2013) R1323–R1330.
[73] G. Yang, G. Istas, S. Höges, M. Yakoub, U. Hendgen-Cotta, T. Rassaf, A. Rodriguez-Mateos, L. Hering, M. Grandoch, E. Mergia, L.C. Rump, J. Stegbauer, Angiotensin-(1-7)-induced Mas receptor activation attenuates atherosclerosis through a nitric oxide-dependent mechanism in apolipoproteinE-KO mice, Pflug. Arch. 470 (4) (2018) 661–667.
[74] J. Jawien, J. Toton-Zuranska, M. Gajda, A. Niepsuj, A. Gebska, K. Kus, M. Suski, G. Pyka-Fosciak, B. Nowak, T.J. Guzik, J. Marcinkiewicz, R. Olszanecki, R. Korbut, Angiotensin-(1-7) receptor Mas agonist ameliorates progress of atherosclerosis in apoE-knockout mice, J. Physiol. Pharmacol. Off. J. Pol. Physiol. Soc. 63 (1) (2012) 77–85.
[75] P. Xu, A.C. Costa-Goncalves, M. Todiras, L.A. Rabelo, W.O. Sampaio, M. M. Moura, S.S. Santos, F.C. Luft, M. Bader, V. Gross, N. Alenina, R.A. Santos, Endothelial dysfunction and elevated blood pressure in MAS gene-deleted mice, Hypertension 51 (2) (2008) 574–580.
[76] C. Savoia, E. Arrabito, R. Parente, C. Nicoletti, L. Madaro, A. Battistoni, A. Filippini, U.M. Steckelings, R.M. Touyz, M. Volpe, Mas receptor activation contributes to the improvement of nitric oxide bioavailability and vascular remodeling during chronic AT1R (Angiotensin Type-1 Receptor) blockade in experimental hypertension, Hypertension 76 (6) (2020) 1753–1761.
[77] B. Fels, K. Kusche-Vihrog, It takes more than two to tango: mechanosignaling of the endothelial surface, Pflug. Arch. 472 (4) (2020) 419–433.
[78] J. Fels, P. Jeggle, K. Kusche-Vihrog, H. Oberleithner, Cortical actin nanodynamics determines nitric oxide release in vascular endothelium, PloS One 7 (7) (2012) e41520.
[79] H. Oberleithner, C. Riethmüller, H. Schillers, G.A. MacGregor, H.E. de Wardener, M. Hausberg, Plasma sodium stiffens vascular endothelium and reduces nitric oxide release, Proc. Natl. Acad. Sci. 104 (41) (2007) 16281–16286.
[80] E. Le Master, R.T. Huang, C. Zhang, Y. Bogachkov, C. Coles, T.P. Shentu, Y. Sheng, I.S. Fancher, C. Ng, T. Christoforidis, P.V. Subbaiah, E. Berdyshev, Z. Qain, D.T. Eddington, J. Lee, M. Cho, Y. Fang, R.D. Minshall, I. Levitan, Proatherogenic flow increases endothelial stiffness via enhanced CD36-mediated

uptake of oxidized low-density lipoproteins, Arterioscler., Thromb., Vasc. Biol. 38 (1) (2018) 64–75.
[81] M. Maase, A. Rygula, M.Z. Pacia, B. Proniewski, L. Mateuszuk, M. Sternak, A. Kaczor, S. Chlopicki, K. Kusche-Vihrog, Combined Raman- and AFM-based detection of biochemical and nanomechanical features of endothelial dysfunction in aorta isolated from ApoE/LDLR-/- mice, Nanomed.: Nanotechnol., Biol., Med. 16 (2019) 97–105.
[82] K.M. Marzec, T.P. Wrobel, A. Rygula, E. Maslak, A. Jasztal, A. Fedorowicz, S. Chlopicki, M. Baranska, Visualization of the biochemical markers of atherosclerotic plaque with the use of Raman, IR and AFM, J. Biophotonics 7 (9) (2014) 744–756.
[83] C.P. Wheeler-Jones, C.E. Farrar, A.A. Pitsillides, Targeting hyaluronan of the endothelial glycocalyx for therapeutic intervention, Curr. Opin. Investig. Drugs 11 (9) (2010) 997–1006.
[84] M. Grandoch, P.L. Bollyky, J.W. Fischer, Hyaluronan: a master switch between vascular homeostasis and inflammation, Circ. Res. 122 (10) (2018) 1341–1343.
[85] F. Hartmann, D.J. Gorski, A.A.C. Newman, S. Homann, A. Petz, K.M. Owsiany, V. Serbulea, Y.Q. Zhou, R.A. Deaton, M. Bendeck, G.K. Owens, J.W. Fischer, SMC-derived hyaluronan modulates vascular SMC phenotype in murine atherosclerosis, Circ. Res. 129 (11) (2021) 992–1005.
[86] N. Nagy, T. Freudenberger, A. Melchior-Becker, K. Röck, M. Ter Braak, H. Jastrow, M. Kinzig, S. Lucke, T. Suvorava, G. Kojda, A.A. Weber, F. Sörgel, B. Levkau, S. Ergün, J.W. Fischer, Inhibition of hyaluronan synthesis accelerates murine atherosclerosis: novel insights into the role of hyaluronan synthesis, Circulation 122 (22) (2010) 2313–2322.
[87] G.F. Mitchell, Arterial stiffness and hypertension, Hypertens. (Dallas, Tex.: 1979) 64 (1) (2014) 13–18.
[88] G.F. Mitchell, Arterial stiffness and hypertension: chicken or egg? Hypertension 64 (2) (2014) 210–214.
[89] P. Boutouyrie, P. Chowienczyk, J.D. Humphrey, G.F. Mitchell, Arterial Stiffness and Cardiovascular Risk in Hypertension, Circ. Res. 128 (7) (2021) 864–886.
[90] K.Rabello Casali, D. Ravizzoni Dartora, M. Moura, M. Bertagnolli, M. Bader, A. Haibara, N. Alenina, M.C. Irigoyen, R.A. Santos, Increased vascular sympathetic modulation in mice with Mas receptor deficiency, J. Renin-angiotensin-Aldosterone Syst. JRAAS 17 (2) (2016), 1470320316643643.
[91] M.M. de Moura, R.A. dos Santos, M.J. Campagnole-Santos, M. Todiras, M. Bader, N. Alenina, A.S. Haibara, Altered cardiovascular reflexes responses in conscious Angiotensin-(1-7) receptor Mas-knockout mice, Peptides 31 (10) (2010) 1934–1939.
[92] P. Xu, A.C. Costa-Goncalves, M. Todiras, L.A. Rabelo, W.O. Sampaio, M. M. Moura, S.S. Santos, F.C. Luft, M. Bader, V. Gross, N. Alenina, R.A. Santos, Endothelial dysfunction and elevated blood pressure in MAS gene-deleted mice, Hypertension 51 (2) (2008) 574–580.
[93] C. Tikellis, R. Brown, G.A. Head, M.E. Cooper, M.C. Thomas, Angiotensin-converting enzyme 2 mediates hyperfiltration associated with diabetes, Am. J. Physiol. Ren. Physiol. 306 (7) (2014) F773–F780.
[94] R.A.Peña Silva, Y. Chu, J.D. Miller, I.J. Mitchell, J.M. Penninger, F.M. Faraci, D. D. Heistad, Impact of ACE2 deficiency and oxidative stress on cerebrovascular function with aging, Stroke 43 (12) (2012) 3358–3363.
[95] L.A. Rabelo, M. Todiras, V. Nunes-Souza, F. Qadri, I.A. Szijártó, M. Gollasch, J. M. Penninger, M. Bader, R.A. Santos, N. Alenina, Genetic deletion of ACE2 induces vascular dysfunction in C57BL/6 mice: role of nitric oxide imbalance and oxidative stress, PloS One 11 (4) (2016) e0150255.
[96] L.A. Benvenuti, R.Y. Onishi, P.S. Gutierrez, M. de Lourdes Higuchi, Different patterns of atherosclerotic remodeling in the thoracic and abdominal aorta, Clinics 60 (5) (2005) 355–360.
[97] D.E. Vaughan, AT(1) receptor blockade and atherosclerosis: hopeful insights into vascular protection, Circulation 101 (13) (2000) 1496–1497.
[98] M. Pellegrin, J. Szostak, K. Bouzourène, J.F. Aubert, A. Berthelot, J. Nussberger, P. Laurant, L. Mazzolai, Running exercise and angiotensin ii type i receptor blocker telmisartan are equally effective in preventing angiotensin ii-mediated vulnerable atherosclerotic lesions, J. Cardiovasc. Pharmacol. Ther. 22 (2) (2017) 159–168.
[99] N. Schlimmer, M. Kratz, M. Böhm, M. Baumhäkel, Telmisartan, ramipril and their combination improve endothelial function in different tissues in a murine model of cholesterol-induced atherosclerosis, Br. J. Pharmacol. 163 (4) (2011) 804–814.
[100] D. Fukuda, S. Enomoto, Y. Hirata, R. Nagai, M. Sata, The angiotensin receptor blocker, telmisartan, reduces and stabilizes atherosclerosis in ApoE and AT1aR double deficient mice, Biomed. Pharmacother. = Biomedecine Pharmacother. 64 (10) (2010) 712–717.
[101] N. Nagy, A. Melchior-Becker, J.W. Fischer, Long-term treatment with the AT1-receptor antagonist telmisartan inhibits biglycan accumulation in murine atherosclerosis, Basic Res. Cardiol. 105 (1) (2010) 29–38.
[102] E. Blessing, M. Preusch, R. Kranzhöfer, R. Kinscherf, N. Marx, M.E. Rosenfeld, B. Isermann, C.M. Weber, J. Kreuzer, J. Gräfe, H.A. Katus, F. Bea, Anti-atherosclerotic properties of telmisartan in advanced atherosclerotic lesions in apolipoprotein E deficient mice, Atherosclerosis 199 (2) (2008) 295–303.
[103] S.J. Hong, S.C. Choi, C.M. Ahn, J.H. Park, J.S. Kim, D.S. Lim, Telmisartan reduces neointima volume and pulse wave velocity 8 months after zotarolimus-eluting stent implantation in hypertensive type 2 diabetic patients, Heart Br. Card. Soc. 97 (17) (2011) 1425–1432.
[104] T. Takaya, S. Kawashima, M. Shinohara, T. Yamashita, R. Toh, N. Sasaki, N. Inoue, K. Hirata, M. Yokoyama, Angiotensin II type 1 receptor blocker telmisartan suppresses superoxide production and reduces atherosclerotic lesion formation in apolipoprotein E-deficient mice, Atherosclerosis 186 (2) (2006) 402–410.
[105] B.H. Li, S.Q. Liao, Y.W. Yin, C.Y. Long, L. Guo, X.J. Cao, Y. Liu, Y. Zhou, C.Y. Gao, L.L. Zhang, J.C. Li, Telmisartan-induced PPARγ activity attenuates lipid accumulation in VSMCs via induction of autophagy, Mol. Biol. Rep. 42 (1) (2015) 179–186.
[106] C. Bian, Y. Wu, P. Chen, Telmisartan increases the permeability of endothelial cells through zonula occludens-1, Biol. Pharm. Bull. 32 (3) (2009) 416–420.
[107] A. Link, M. Lenz, D. Legner, M. Böhm, G. Nickenig, Telmisartan inhibits beta2-integrin MAC-1 expression in human T-lymphocytes, J. Hypertens. 24 (9) (2006) 1891–1898.
[108] Y.J. Hwang, J.H. Park, D.H. Cho, Activation of AMPK by telmisartan decreases basal and PDGF-stimulated VSMC proliferation via inhibiting the mTOR/p70S6K signaling axis, J. Korean Med. Sci. 35 (35) (2020) e289.
[109] H. Ikejima, T. Imanishi, H. Tsujioka, A. Kuroi, K. Kobayashi, M. Shiomi, Y. Muragaki, S. Mochizuki, M. Goto, K. Yoshida, T. Akasaka, Effects of telmisartan, a unique angiotensin receptor blocker with selective peroxisome proliferator-activated receptor-gamma-modulating activity, on nitric oxide bioavailability and atherosclerotic change, J. Hypertens. 26 (5) (2008) 964–972.
[110] Y.K. Chan, H. El-Nezami, Y. Chen, K. Kinnunen, P.V. Kirjavainen, Probiotic mixture VSL#3 reduce high fat diet induced vascular inflammation and atherosclerosis in ApoE(-/-) mice, AMB Express 6 (1) (2016) 61.
[111] Y.K. Chan, M.S. Brar, P.V. Kirjavainen, Y. Chen, J. Peng, D. Li, F.C. Leung, H. El-Nezami, High fat diet induced atherosclerosis is accompanied with low colonic bacterial diversity and altered abundances that correlates with plaque size, plasma A-FABP and cholesterol: a pilot study of high fat diet and its intervention with Lactobacillus rhamnosus GG (LGG) or telmisartan in ApoE(-/-) mice, BMC Microbiol. 16 (1) (2016) 264.
[112] J.Y. Chen, Y.P. Wu, C.Y. Li, H.F. Jheng, L.Z. Kao, C.C. Yang, S.Y. Leu, I.C. Lien, W. T. Weng, H.C. Tai, Y.W. Chiou, M.J. Tang, P.J. Tsai, Y.S. Tsai, PPARγ activation improves the microenvironment of perivascular adipose tissue and attenuates aortic stiffening in obesity, J. Biomed. Sci. 28 (1) (2021) 22.
[113] T. Matsumura, H. Kinoshita, N. Ishii, K. Fukuda, H. Motoshima, T. Senokuchi, K. Taketa, S. Kawasaki, T. Nishimaki-Mogami, T. Kawada, T. Nishikawa, E. Araki, Telmisartan exerts antiatherosclerotic effects by activating peroxisome proliferator-activated receptor-γ in macrophages, Arterioscler., Thromb., Vasc. Biol. 31 (6) (2011) 1268–1275.
[114] K. Yamamoto, M. Ohishi, C. Ho, T.W. Kurtz, H. Rakugi, Telmisartan-induced inhibition of vascular cell proliferation beyond angiotensin receptor blockade and peroxisome proliferator-activated receptor-gamma activation, Hypertension 54 (6) (2009) 1353–1359.
[115] V. Tiyerili, U.M. Becher, A. Aksoy, D. Lütjohann, S. Wassmann, G. Nickenig, C. F. Mueller, AT1-receptor-deficiency induced atheroprotection in diabetic mice is partially mediated via PPARγ, Cardiovasc. Diabetol. 12 (2013) 30.
[116] L. Klinghammer, K. Urschel, I. Cicha, P. Lewczuk, D. Raaz-Schrauder, S. Achenbach, C.D. Garlichs, Impact of telmisartan on the inflammatory state in patients with coronary atherosclerosis–influence on IP-10, TNF-α and MCP-1, Cytokine 62 (2) (2013) 290–296.
[117] K. Shelbaya, V. Arthur, Y. Yang, P. Dorbala, L. Buckley, B. Claggett, H. Skali, L. Dufresne, T.Y. Yang, J.C. Engert, G. Thanassoulis, J. Floyd, T.R. Austin, A. Bortnick, J. Kizer, R.C.C. Freitas, S.A. Singh, E. Aikawa, R.C. Hoogeveen, C. Ballantyne, B. Yu, J. Coresh, M.J. Blaha, K. Matsushita, A.M. Shah, Large-scale proteomics identifies novel biomarkers and circulating risk factors for aortic stenosis, J. Am. Coll. Cardiol. 83 (5) (2024) 577–591.
[118] I. Goncalves, E. Bengtsson, H.M. Colhoun, A.C. Shore, C. Palombo, A. Natali, A. Edsfeldt, P. Dunér, G.N. Fredrikson, H. Björkbacka, G. Östling, K. Aizawa, F. Casanova, M. Persson, K. Gooding, D. Strain, F. Khan, H.C. Looker, F. Adams, J. Belch, S. Pinnoli, E. Venturi, M. Kozakova, L.M. Gan, V. Schnecke, J. Nilsson, Elevated plasma levels of MMP-12 are associated with atherosclerotic burden and symptomatic cardiovascular disease in subjects with type 2 diabetes, Arterioscler., Thromb. Vasc. Biol. 35 (7) (2015) 1723–1731.
[119] S. Yamada, K.Y. Wang, A. Tanimoto, J. Fan, S. Shimajiri, S. Kitajima, M. Morimoto, M. Tsutsui, T. Watanabe, K. Yasumoto, Y. Sasaguri, Matrix metalloproteinase 12 accelerates the initiation of atherosclerosis and stimulates the progression of fatty streaks to fibrous plaques in transgenic rabbits, Am. J. Pathol. 172 (5) (2008) 1419–1429.
[120] S.L. Liu, Y.H. Bae, C. Yu, J. Monslow, E.A. Hawthorne, P. Castagnino, E. Branchetti, G. Ferrari, S.M. Damrauer, E. Puré, R.K. Assoian, Matrix metalloproteinase-12 is an essential mediator of acute and chronic arterial stiffening, Sci. Rep. 5 (2015) 17189.
[121] F. Krueger, K. Kappert, A. Foryst-Ludwig, F. Kramer, M. Clemenz, A. Grzesiak, M. Sommerfeld, J.P. Frese, A. Greiner, U. Kintscher, T. Unger, E. Kaschina, AT1-receptor blockade attenuates outward aortic remodeling associated with diet-induced obesity in mice, Clin. Sci. 131 (15) (2017) 1989–2005.
[122] L.J. Du, J.Y. Sun, W.C. Zhang, Y. Liu, Y. Liu, W.Z. Lin, T. Liu, H. Zhu, Y.L. Wang, S. Shao, L.J. Zhou, B.Y. Chen, H. Lu, R.G. Li, F. Jia, S.Z. Duan, NCOR1 maintains the homeostasis of vascular smooth muscle cells and protects against aortic aneurysm, Cell Death Differ. 30 (3) (2023) 618–631.
[123] K. Ji, Y. Zhang, F. Jiang, L. Qian, H. Guo, J. Hu, L. Liao, J. Tang, Exploration of the mechanisms by which 3,4-benzopyrene promotes angiotensin II-induced abdominal aortic aneurysm formation in mice, J. Vasc. Surg. 59 (2) (2014) 492–499.
[124] K. Gopal, P. Nagarajan, J. Jedy, A.T. Raj, S.K. Gnanaselvi, P. Jahan, Y. Sharma, E. M. Shankar, J.M. Kumar, β-carotene attenuates angiotensin ii-induced aortic aneurysm by alleviating macrophage recruitment in Apoe(-/-) mice, PloS One 8 (6) (2013) e67098.
[125] A. Kunath, J. Unosson, M. Friederich-Persson, N. Bjarnegård, M. Becirovic-Agic, M. Björck, K. Mani, A. Wanhainen, D. Wågsäter, Inhibition of angiotensin-induced

aortic aneurysm by metformin in apolipoprotein E-deficient mice, JVS-Vasc. Sci. 2 (2021) 33–42.
[126] H. Ma, Y.L. Wang, N.H. Hei, J.L. Li, X.R. Cao, B. Dong, W.J. Yan, AVE0991, a nonpeptide angiotensin-(1-7) mimic, inhibits angiotensin II-induced abdominal aortic aneurysm formation in apolipoprotein E knockout mice, J. Mol. Med. 98 (4) (2020) 541–551.
[127] G.S. Magalhães, J.F. Gregório, K.E. Ramos, A.T.P. Cançado-Ribeiro, I.F. Baroni, L. S. Barcelos, V. Pinho, M.M. Teixeira, R.A.S. Santos, M.G. Rodrigues-Machado, M. J. Campagnole-Santos, Treatment with inhaled formulation of angiotensin-(1-7) reverses inflammation and pulmonary remodeling in a model of chronic asthma, Immunobiology 225 (3) (2020) 151957.
[128] Z. Wang, W. Huang, F. Ren, L. Luo, J. Zhou, D. Huang, M. Jiang, H. Du, J. Fan, L. Tang, Characteristics of Ang-(1-7)/mas-mediated amelioration of joint inflammation and cardiac complications in mice with collagen-induced arthritis, Front. Immunol. 12 (2021) 655614.
[129] M.C. Lavigne, P. Thakker, J. Gunn, A. Wong, J.S. Miyashiro, A.M. Wasserman, S. Q. Wei, J.W. Pelker, M. Kobayashi, M.J. Eppihimer, Human bronchial epithelial cells express and secrete MMP-12, Biochem. Biophys. Res. Commun. 324 (2) (2004) 534–546.
[130] W. Li, J. Li, P. Hao, W. Chen, X. Meng, H. Li, Y. Zhang, C. Zhang, J. Yang, Imbalance between angiotensin II and angiotensin-(1-7) in human coronary atherosclerosis, J. Renin-angiotensin-Aldosterone Syst.: JRAAS 17 (3) (2016).
[131] L. Roth, M. Rombouts, D.M. Schrijvers, W. Martinet, G.R. De Meyer, Cholesterol-independent effects of atorvastatin prevent cardiovascular morbidity and mortality in a mouse model of atherosclerotic plaque rupture, Vasc. Pharmacol. 80 (2016) 50–58.
[132] M.L. Zhu, R.L. Sun, H.Y. Zhang, F.R. Zhao, G.P. Pan, C. Zhang, P. Song, P. Li, J. Xu, S. Wang, Y.L. Yin, Angiotensin II type 1 receptor blockers prevent aortic arterial stiffness in elderly patients with hypertension, Clin. Exp. Hypertens. 41 (7) (2019) 657–661.
[133] X.J. Yu, Y.Q. Huang, Z.X. Shan, J.N. Zhu, Z.Q. Hu, L. Huang, Y.Q. Feng, Q. S. Geng, MicroRNA-92b-3p suppresses angiotensin II-induced cardiomyocyte hypertrophy via targeting HAND2, Life Sci. 232 (2019) 116635.
[134] A. Pautz, H. Li, H. Kleinert, Regulation of NOS expression in vascular diseases, Front. Biosci. 26 (5) (2021) 85–101.
[135] M. Myojo, D. Nagata, D. Fujita, A. Kiyosue, M. Takahashi, H. Satonaka, Y. Morishita, T. Akimoto, R. Nagai, I. Komuro, Y. Hirata, Telmisartan activates endothelial nitric oxide synthase via Ser1177 phosphorylation in vascular endothelial cells, PloS One 9 (5) (2014) e96948.
[136] L. Uthman, A. Homayr, R.P. Juni, E.L. Spin, R. Kerindongo, M. Boomsma, M. W. Hollmann, B. Preckel, P. Koolwijk, V.W.M. van Hinsbergh, C.J. Zuurbier, M. Albrecht, N.C. Weber, Empagliflozin and dapagliflozin reduce ros generation and restore NO bioavailability in tumor necrosis factor α-stimulated human coronary arterial endothelial cells, Cell. Physiol. Biochem. Int. J. Exp. Cell. Physiol. Biochem. Pharmacol. 53 (5) (2019) 865–886.
[137] H. Grimm, J. Kretzschmar, M.D. Cook, M.D. Brown, The effects of exercise, aspirin, and celecoxib in an atherogenic environment, Med. Sci. Sports Exerc. 50 (10) (2018) 2033–2039.
[138] M. Bader, ACE2, angiotensin-(1–7), and Mas: the other side of the coin, Pflug. Arch. 465 (1) (2013) 79–85.
[139] M. Paar, H. Pavenstädt, K. Kusche-Vihrog, V. Drüppel, H. Oberleithner, K. Kliche, Endothelial sodium channels trigger endothelial salt sensitivity with aging, Hypertension 64 (2) (2014) 391–396.